J|A|C|S
ARTICLES
Published on Web 03/25/2004

Light-Emitting Tridentate Cyclometalated Platinum(II) Complexes Containing σ-Alkynyl Auxiliaries: Tuning of Photo- and Electrophosphorescence

Wei Lu,[†] Bao-Xiu Mi,[‡] Michael C. W. Chan,[†] Zheng Hui,[†] Chi-Ming Che,*[,†] Nianyong Zhu,[†] and Shuit-Tong Lee[‡]

Contribution from the Department of Chemistry and HKU-CAS Joint Laboratory on New Materials, The University of Hong Kong, Pokfulam Road, Hong Kong SAR, China, and Centre of Super-Diamond and Advanced Films and Department of Physics and Materials Science, City University of Hong Kong, Kowloon, Hong Kong SAR, China

Received December 17, 2003; E-mail: cmche@hku.hk

Abstract: The synthesis and structural, photophysical, electrochemical, and electroluminescent properties of a class of platinum(II) complexes bearing σ-alkynyl ancillary ligands, namely [(C^N^N)Pt(C≡C)$_n$R] [H(C^N^N) = 6-aryl-2,2′-bipyridine; $n = 1-4$; R = aryl, alkyl, or trimethylsilyl], have been studied. Substituents with different steric and electronic properties were introduced into the tridentate cyclometalating and arylacetylide ligands, and the π-conjugation length of the oligoynyl moiety was homologously extended from ethynyl to octatetraynyl. The X-ray crystal structures of several derivatives confirm the Pt−(C≡C) ligation and reveal various intermolecular interactions, such as $\pi-\pi$, Pt···Pt, and C−H···F−C. The complexes display good thermal stability and intense phosphorescence in fluid and glassy solutions with high quantum yields and microsecond lifetimes. Their emission energies are sensitive to solvent polarity, the electronic affinities of the substituents on both the cyclometalating and arylacetylide groups, and the length of the oligoynyl ligand. By choosing appropriate cyclometalating and σ-alkynyl ligands, the emission color of this class of platinum(II) complexes can be tuned from green-yellow to saturated red. In addition to ^{3}MLCT [Pt(5d) → π*(C^N^N)] and ^{3}IL(C^N^N), intriguing ^{3}IL(alkynyl) excited states localized on −(C≡C)$_4$− and −(C≡Cpyrenyl-1) moieties that afford narrow-bandwidth emissions have been observed. Selected Pt(II) complexes were doped into the emissive region of multilayer, vapor-deposited organic light-emitting diodes. The tunable electrophosphorescence energy resembles that recorded in fluid solutions for these emitters, and the devices exhibit high luminance and efficiencies (up to 4.2 cd A^{-1}).

Introduction

The scope and diversity of studies on transition metal σ-alkynyl complexes in the realm of material science have continued to expand since the initiate report on soluble [Pt(P^{n}Bu$_3$)$_2$]-bearing oligoyne polymers in 1975.[1] Acetylide and polyyne moieties, as rigid π-conjugated bridging components, facilitate a wide range of photorelated processes, including triplet energy transfer, electron (or hole) transfer, photon migration, and electron delocalization, while maintaining strict stereochemical integrity.[2] There has been particular interest in platinum(II) σ-alkynyl complexes for nonlinear optics, liquid crystals, low-dimension conductors, photovoltaic devices, and supramolecular hosts applications due to their chemical and structural stability. However, investigations into the light-emitting characteristics of these materials are partly hindered by the lack of luminescence under ambient conditions for Pt(II) σ-alkynyl derivatives supported by phosphine ligands.[3] Recently, Raithby and co-workers reported a blue-luminescent [Pt(P^{n}Bu$_3$)$_2$]-based polymer with acetylide ligands containing low-lying π* orbitals in the main chain, and the emission was assigned to triplet intraligand (IL) charge-transfer excited state of the bridging acetylide group.[4] Ligation of oligopyridines,

[†] The University of Hong Kong.
[‡] City University of Hong Kong.

(1) (a) Fujikura, Y.; Sonogashira, K.; Hagihara, N. *Chem. Lett.* **1975**, 1067−1070. (b) Sonogashira, K.; Takahashi, S.; Hagihara, N. *Macromolecules* **1977**, *10*, 879−880.
(2) (a) Manna, J.; John, K. D.; Hopkins, M. D. *Adv. Organomet. Chem.* **1995**, *38*, 79−154. (b) Tour, J. M. *Chem. Rev.* **1996**, *96*, 537−554. (c) Paul, F.; Lapinte, C. *Coord. Chem. Rev.* **1998**, *178−180*, 431−509. (d) Lavastre, O.; Plass, J.; Bachmann, P.; Guesmi, S.; Moinet, C.; Dixneuf, P. H. *Organometallics* **1997**, *16*, 184−189. (e) Touchard, D.; Haquette, P.; Daridor, A.; Romero, A.; Dixneuf, P. H. *Organometallics* **1998**, *17*, 3844−3852. (f) John, K. D.; Hopkins, M. D. *Chem. Commun.* **1999**, 589−590. (g) Long, N. J. In *Optoelectronic Properties of Inorganic Compounds*; Roundhill, D. M., Fackler, J. P., Jr., Eds.; Plenum Press: New York, 1999, Chapter 4. (h) Schwab, P. F. H.; Levin, M. D.; Michl, J. *Chem. Rev.* **1999**, *99*, 1863−1934. (i) Nguyen, P.; Gomez-Elipe, P.; Manners, I. *Chem. Rev.* **1999**, *99*, 1515−1548. (j) Martin, R. E.; Diederich, F. *Angew. Chem., Int. Ed. Engl.* **1999**, *38*, 1350−1377. (k) Swager, T. M. *Acc. Chem. Res.* **1998**, *31*, 201. (l) Bunz, U. H. F. *Chem. Rev.* **2000**, *100*, 1605−1644. (m) Long, N. J.; Williams, C. K. *Angew. Chem., Int. Ed.* **2003**, *42*, 2586−2617.
(3) (a) Lewis, J.; Khan, M. S.; Kakkar, A. K.; Johnson, B. F. G.; Marder, T. B.; Fyfe, H. B.; Wittmann, F.; Friend, R. H.; Dray, A. E. *J. Organomet. Chem.* **1992**, *425*, 165−176. (b) Frapper, G.; Kertesz, M. *Inorg. Chem.* **1993**, *32*, 732−740. (c) Bunten, K. A.; Kakkar, A. K. *Macromolecules* **1996**, *29*, 2885−2893. (d) Chawdhury, N.; Köhler, A.; Friend, R. H.; Wong, W. Y.; Lewis, J.; Younus, M.; Raithby, P. R.; Corcoran, T. C.; Al-Mandhary, M. R. A.; Khan, M. S. *J. Chem. Phys.* **1999**, *110*, 4963−4970. (e) Wilson, J. S.; Köhler, A.; Friend, R. H.; Al Suti, M. K.; Al -Mandhary, M. R. A.; Khan, M. S.; Raithby, P. R. *J. Chem. Phys.* **2000**, *113*, 7627−7634.

10.1021/ja0317776 CCC: $27.50

which also feature low-lying π^* orbitals, is another way to harness the luminescence of Pt(II) σ-alkynyl species. In 1994, our research group reported the first luminescent Pt(II) acetylide complex with aromatic diimine ligands, namely [Pt(phen)(C≡CPh)$_2$] (phen = 1,10-phenanthroline), which exhibits intense triplet [5d(Pt) → π^*(phen)] metal-to-ligand charge transfer (MLCT) emission in fluid solution at room temperature.[5] Subsequent studies have improved the synthetic procedure and probed the excited-state properties of [Pt(α-diimine)(C≡CAr)$_2$] complexes through systematic modification of both the diimine and acetylide auxiliaries.[6] Intriguingly, these complexes have recently been shown to be promising materials in organic light-emitting diodes (OLEDs)[7] as well as photoinduced charge-separation systems.[8]

There has been tremendous impetus to develop OLEDs using organic or metal-organic compounds as emitting materials since the report in 1987 by Tang and Van Slyke of a electroluminescent (EL) device using Alq_3 (q = 8-quinolinate) as the fluorescent emitter.[9] Recent progress has shown that phosphorescent materials should in principle be superior to fluorescent substrates for small-molecule OLED applications.[10] This is because efficient phosphorescent emitters doped into fluorescent host materials can potentially harvest both singlet and triplet excitons upon electron−hole recombination from electrical excitation. The [Ir(C^N)$_3$] (HC^N = 2-phenylpyridine) complex and its derivatives has been one of the most widely studied class of electrophosphorescent emitters containing a heavy transition metal since it was first described in 2000 by Baldo, Thompson, and Forrest.[11] Efficiencies of OLEDs were dramatically increased to, for example, 15.4 ± 0.2% and almost 100% for external and internal quantum efficiency respectively, by employing this green emitter in a multilayer heterostructure.[10e] Furthermore, it has been reported that chemical modifications of tris- and bis-cyclometalated iridium(III) derivatives can afford substantial improvements.[10d] For instance, fluorinated analogues can reduce triplet−triplet annihilation processes and increase their sublimability,[12] introduction of bulky groups can decrease the self-quenching of emitters at high doping levels,[13] the use of fluorene-modified (C^N) ligands yields crystallization-resistant materials that can be incorporated into single layer OLEDs,[14] expanding the π-conjugation of the (C^N) ligands can result in enhanced device performances,[15] and the employment of facial isomers leads to blue-shifted emissions and higher quantum efficiencies compared to meridional analogues.[10f] Color-tuning of the emission is possible and blue to red electrophosphorescence with excellent efficiencies based on these derivatives have been achieved.[10d] All endeavors to tune the photophysical and electroluminescent properties of the bis- and tris-cyclometalated iridium complexes have been focused on varying the donor and/or acceptor groups on the (C^N) ligands whereas the third bidentate auxiliary, such as acetylacetonate (acac), is apparently ineffective in modifying the triplet intraligand-dominated excited state of Ir(III) complexes (Scheme 1).

Scheme 1. Excited-State Tuning for Phosphorescent Ir(III)-(predominantly IL) and Pt(II)- (MLCT and IL) Based Complexes through Ligand Modification

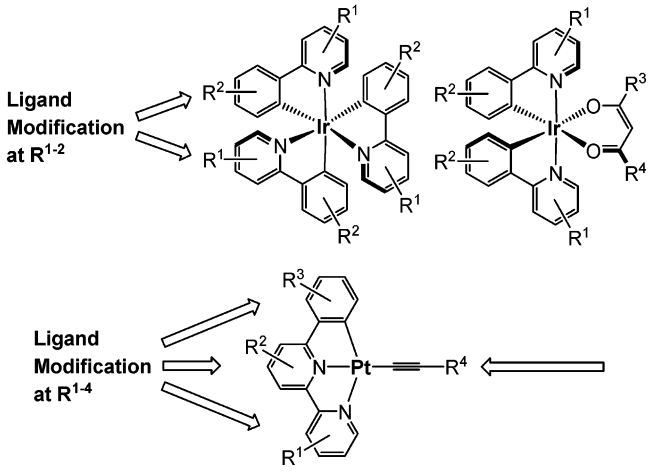

Our present study aims to develop high-efficiency emitters based on Pt(II) σ-alkynyl complexes. The tridentate cyclometalated Pt(II) lumophores [Pt(C^N^N)][16] are chosen because of their superior emissive properties compared to the 2,2′:6′,2″-terpyridine (tpy)[17] and (C^N^C) (HC^N^CH = 2,6-diphenylpyridine)[18] congeners. The anionic σ-alkynyl ligand affords

(4) Younus, M.; Köhler, A.; Cron, S.; Chawdhury, N.; Al -Mandhary, M. R. A.; Khan, M. S.; Lewis, J.; Long, N. J.; Friend, R. H.; Raithby, P. R. *Angew. Chem., Int. Ed. Engl.* **1998**, *37*, 3036−3039.
(5) Chan, C. W.; Cheng, L. K.; Che, C. M. *Coord. Chem. Rev.* **1994**, *132*, 87−97.
(6) (a) Connick, W. B.; Geiger, D.; Eisenberg, R. *Inorg. Chem.* **1999**, *38*, 3264−3265. (b) Hissler, M.; Connick, W. B.; Geiger, D. K.; McGarrah, J. E.; Lipa, D.; Lachicotte, R. J.; Eisenberg, R. *Inorg. Chem.* **2000**, *39*, 447−457. (c) Whittle, C. E.; Weinstein, J. A.; George, M. W.; Schanze, K. S. *Inorg. Chem.* **2001**, *40*, 4053−4062. (d) Wadas, T. J.; Lachicotte, R. J.; Eisenberg, R. *Inorg. Chem.* **2003**, *42*, 3772−3778. (e) Pomestchenko, I. E.; Luman, C. R.; Hissler, M.; Ziessel, R.; Castellano, F. N. *Inorg. Chem.* **2003**, *42*, 1394−1396. (f) Fernandez, S.; Fornies, J.; Gil, B.; Gomez, J.; Lalinde, E. *J. Chem. Soc., Dalton Trans.* **2003**, 822−830.
(7) Chan, S. C.; Chan, M. C. W.; Che, C. M.; Wang, Y.; Cheung, K. K.; Zhu, N. Y. *Chem. Eur. J.* **2001**, *7*, 4180−4190.
(8) McGarrah, J. E.; Kim, Y. J.; Hissler, M.; Eisenberg, R. *Inorg. Chem.* **2001**, *40*, 4510−4511.
(9) Tang, C. W.; Van Slyke, S. A. *Appl. Phys. Lett.* **1987**, *51*, 193−195.
(10) (a) Baldo, M. A.; O'Brien, D. F.; You, Y.; Shoustikov, A.; Sibley, S.; Thompson, M. E.; Forrest, S. R. *Nature* **1998**, *395*, 151−154. (b) Ma, Y. G.; Zhang, H. Y.; Shen, J. C.; Che, C. M. *Synth. Met.* **1998**, *94*, 245−248. (c) Adachi, C.; Baldo, M. A.; Forrest, S. R.; Thompson, M. E. *Appl. Phys. Lett.* **2000**, *77*, 904−906. (d) Lamansky, S.; Djurovich, P.; Murphy, D.; Abdel-Razzaq, F.; Lee, H. E.; Adachi, C.; Burrows, P.; Forrest, S. R.; Thompson, M. E. *J. Am. Chem. Soc.* **2001**, *123*, 4304−4312. (e) Adachi, C.; Baldo, M. A.; Forrest, S. R.; Lamansky, S.; Thompson, M. E. Kwong, R. C. *Appl. Phys. Lett.* **2001**, *78*, 1622−1624. (f) Tamayo, A. B.; Alleyne, B. D.; Djurovich, P.; Lamansky, S.; Tsyba, I.; Ho, N. N.; Bau, R.; Thompson, M. E. *J. Am. Chem. Soc.* **2003**, *125*, 7377−7387. (g) Nazeeruddin, M. K.; Humphry-Baker, R.; Berner, D.; Rivier, S.; Zuppiroli, L.; Graetzel, M. *J. Am. Chem. Soc.* **2003**, *125*, 8790−8797.
(11) Baldo, M. A.; Thompson, M. E.; Forrest, S. R. *Nature* **2000**, *403*, 750−753.
(12) Grushin, V. V.; Herron, N.; LeCloux, D. D.; Marshall, W. J.; Petrov, V. A.; Wang, Y. *Chem. Commun.* **2001**, 1494−1495.
(13) Xie, H. Z.; Liu, M. W.; Wang, O. Y.; Zhang, X. H.; Lee, C. S.; Hung, L..S.; Lee, S. T.; Teng, P. F.; Kwong, H. L.; Hui, Z.; Che, C. M. *Adv. Mater.* **2001**, *13*, 1245−1248.
(14) Ostrowski, J. C.; Robinson, M. R.; Heeger, A. J.; Bazan, G. C. *Chem. Commun.* **2002**, 784−785.
(15) (a) Duan, J. P.; Sun, P. P.; Cheng, C. H. *Adv. Mater.* **2003**, *15*, 224−228. (b) Su, Y. J.; Huang, H. L.; Li, C. L.; Chien, C. H.; Tao, Y. T.; Chou, P. T.; Datta, S.; Liu, R. S. *Adv. Mater.* **2003**, *15*, 884−888. (c) Tsuboyama, A.; Iwawaki, H.; Furugori, M.; Mukaide, T.; Kamatani, J.; Igawa, S.; Moriyama, T.; Miura, S.; Takiguchi, T.; Okada, S.; Hoshino, M.; Ueno, K. *J. Am. Chem. Soc.* **2003**, *125*, 12 971−12 979.
(16) (a) Chan, C. W.; Lai, T. F.; Che, C. M.; Peng, S. M. *J. Am. Chem. Soc.* **1993**, *115*, 11 245−11 253. (b) Cheung, T. C.; Cheung, K. K.; Peng, S. M.; Che, C. M. *J. Chem. Soc., Dalton Trans.* **1996**, 1645−1651. (c) Neve, F.; Ghedini, M.; Crispini, A. *J. Chem. Soc., Chem. Commun.* **1996**, 2463−2464. (d) Lai, S. W.; Chan, M. C. W.; Cheung, T. C.; Peng, S. M.; Che, C. M. *Inorg. Chem.* **1999**, *38*, 4046−4055. (e) Lai, S. W.; Chan, M. C. W.; Cheung, K. K.; Che, C. M. *Organometallics* **1999**, *18*, 3327−3336. (f) Yip, J. H. K.; Suwarno; Vittal, J. J. *Inorg. Chem.* **2000**, *39*, 3537−3543.
(17) (a) Arena, G.; Calogero, G.; Campagna, S.; Scolaro, L. M.; Ricevuto, V.; Romeo, R. *Inorg. Chem.* **1998**, *37*, 2763−2769. (b) Michalec, J. F.; Bejune, S. A.; McMillin, D. R. *Inorg. Chem.* **2000**, *39*, 2708−2709. (c) Yam, V. W. W.; Tang, R. P. L.; Wong, K. M. C.; Ko, C. C.; Cheung, K. K. *Inorg. Chem.* **2001**, *40*, 571−574.

Chart 1

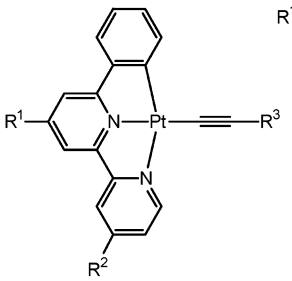

$R^1 = R^2 = H$		
	$R^3 = Ph$	**1**
	C_6H_4-4-CH_3	**2**
	C_6H_4-4-OCH_3	**3**
	C_6H_4-4-Cl	**4**
	C_6H_4-4-F	**5**
	C_6H_4-4-NO_2	**6**
	C_6F_5	**7**
	$C{\equiv}CPh$	**8**
	$C(CH_3)_3$	**9**
	$Si(CH_3)_3$	**10**
	$C{\equiv}CSi(CH_3)_3$	**11**
	$C{\equiv}C{-}C{\equiv}CSi(CH_3)_3$	**12**
	$C{\equiv}C{-}C{\equiv}C{-}C{\equiv}CSi(CH_3)_3$	**13**
$R^2 = H$, $R^3 = Ph$		
	$R^1 = Ph$	**14**
	4-$CH_3C_6H_4$	**15**
	4-$CH_3OC_6H_4$	**16**
	4-ClC_6H_4	**17**
	4-$NO_2C_6H_4$	**18**
$R^1 = R^2 = {}^t$Bu		
	$R^3 = Ph$	**19**
	C_6F_5	**20**
	pyrenyl-1	**21**
$R^1 = EtO_2C$, $R^2 = H$		
	$R^3 = Ph$	**22**
	C_6F_5	**23**

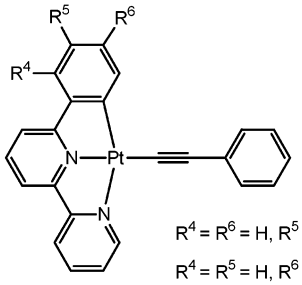

$R^4 = R^6 = H$, $R^5 = CH_3$	**24**
$R^4 = R^5 = H$, $R^6 = CH_3$	**25**
$R^4 = R^5 = H$, $R^6 = CF_3$	**26**
$R^5 = H$, $R^4 = R^6 = F$	**27**

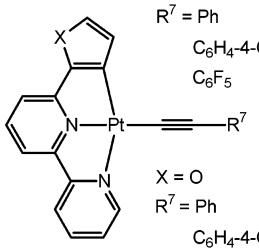

X = S		
	$R^7 = Ph$	**28**
	C_6H_4-4-CH_3	**29**
	C_6F_5	**30**
X = O		
	$R^7 = Ph$	**31**
	C_6H_4-4-CH_3	**32**
	C_6F_5	**33**

neutrality to the [Pt(C^N^N)] moiety and is envisaged to modulate their photophysical properties by (1) destabilizing nonradiative ligand-field transitions that are inherent to this class of compounds and (2) modifying the properties of the triplet excited state [normally Pt $\rightarrow$ π^*(cyclometalating ligand)] through π-bonding conjugation between Pt(II) and the σ-alkynyl auxiliary. We have previously communicated that these materials can be vacuum-deposited into multilayer OLEDs to emit yellow to red light with excellent efficiencies.[19] We now report that extensive modifications of both the tridentate and σ-alkynyl ligands in these complexes can result in subtle tuning of their structural, photophysical and luminescent characteristics and provide a novel family of electrophosphorescent emitters. In 2002, Thompson and Forrest reported the employment of the blue luminescent Pt(II) complex [4′,6′-F_2-(C^N)Pt(acac)] [4′,6′-F_2-(HC^N) = 2-(4′,6′-difluorophenyl)pyridine], which displays orange-red excimeric emission, as a dopant in white light OLEDs.[20]

Results

Synthesis. In this work, substituents with a variety of steric and electronic properties were introduced into the potentially tridentate cyclometalating ligands. The sterically encumbered 6-phenyl-4,4′-bis(*tert*-butyl)-2,2′-bipyridine was prepared from 4,4′-bis(*tert*-butyl)-2,2′-bipyridine through nucleophilic addition of phenyllithium and subsequent oxidation by MnO_2.[21] The other

Scheme 2. Synthesis of the Cyclometalated Pt(II) σ-Alkynyl Complexes

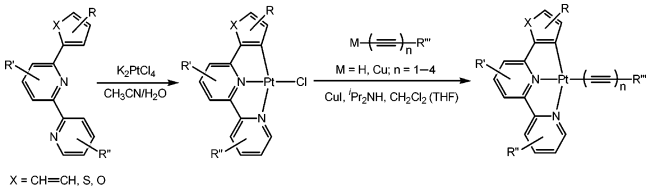

6-aryl-2,2′-bypyridine ligands were obtained using Kröhnke's syntheses for oligopyridines,[22] that is, condensation between acalkylpyridinium salts and α,β-unsaturated ketones in the presence of ammonium acetate in methanol. 4-Ethoxycarbonyl-6-phenyl-2,2′-bipyridine was prepared by refluxing 4-hydroxycarbonyl-6-phenyl-2,2′-bipyridine[23] in ethanol in the presence of concentrated sulfuric acid.

The cyclometalated Pt(II) chloride precursors were synthesized by refluxing the 6-aryl-2,2′-bypyridine ligands and K_2PtCl_4 in CH_3CN/H_2O (1/1, v/v), a method originally developed by Constable and co-workers[24] (Scheme 2). In this work, Pt(II) acetylide complexes (Chart 1) derived from these precursors were prepared by employing Sonogashira's conditions (terminal alkynes, CuI/^{i}Pr_2NH/CH_2Cl_2), which resulted in simple workup and purification procedures. The terminal oligoynes required for **12** and **13** were prepared in situ due to their instability toward heat and light. Thus, the compound $Me_3Si(C{\equiv}C)_nSiMe_3$ (n =

(18) Lu, W.; Chan, M. C. W.; Cheung, K. K.; Che, C. M. *Organometallics* **2001**, *20*, 2477−2486.
(19) Lu, W.; Mi, B. X.; Chan, M. C. W.; Hui, Z.; Zhu, N. Y.; Lee, S. T.; Che, C. M. *Chem. Commun.* **2002**, 206−207.
(20) (a) D′Andrade, B. W.; Brooks, J.; Adamovich, V.; Thompson, M. E.; Forrest, S. R. *Adv. Mater.* **2002**, *14*, 1032−1036. (b) Brooks, J.; Babayan, Y.; Lamansky, S.; Djurovich, P. I.; Tsyba, I.; Bau, R.; Thompson, M. E. *Inorg. Chem.* **2002**, *41*, 3055−3066. (c) Adamovich, V.; Brooks, J.; Tamayo, A.; Alexander, A. M.; Djurovich, P. I.; D'Andrade, B. W.; Adachi, C.; Forrest, S. R.; Thompson, M. E. *New J. Chem.* **2002**, *26*, 1171−1178.
(21) Goodman, M. S.; Hamilton, A. D.; Weiss, J. *J. Am. Chem. Soc.* **1995**, *117*, 8447−8455.
(22) Kröhnke, F. *Synthesis* **1976**, 1−24.
(23) Neve, F.; Crispini, A.; Di Pietro, C.; Campagna, S. *Organometallics* **2002**, *21*, 3511−3518.
(24) (a) Constable, E. C.; Henney, R. P. G.; Leese, T. A.; Tocher, D. A. *J. Chem. Soc., Chem. Commun.* **1990**, 513−515. (b) Constable, E. C.; Henney, R. P. G.; Leese, T. A.; Tocher, D. A. *J. Chem. Soc., Dalton Trans.* **1990**, 443−449. (c) Constable, E. C.; Henney, R. P. G.; Raithby, P. R.; Sousa, L. R. *J. Chem. Soc., Dalton Trans.* **1992**, 2251−2258.

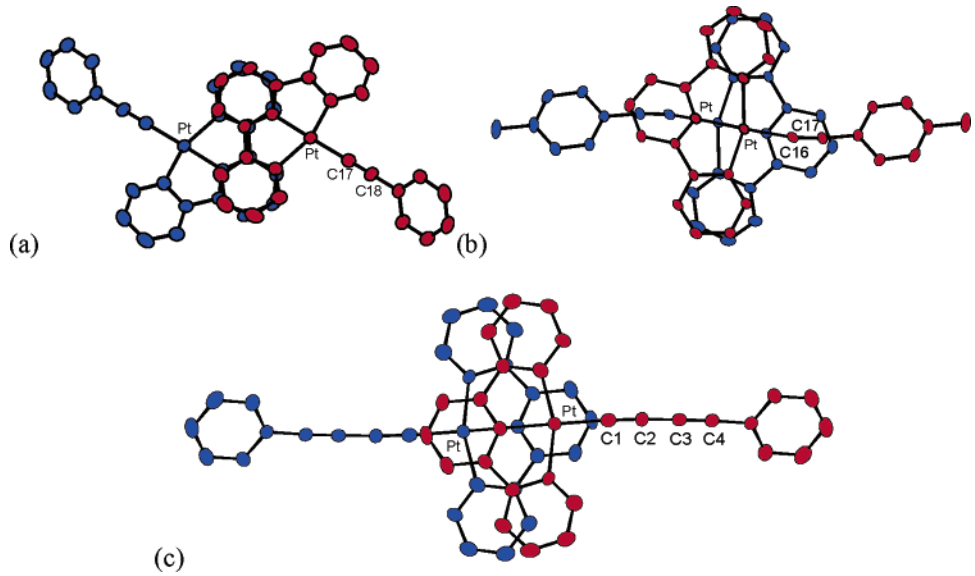

Figure 1. Crystal packing diagrams of **1** (a), **2** (b), and **8** (c), illustrating intermolecular contacts.

3,[25] 4,[26] respectively) was monodesilylated with MeLi in THF in the presence of CuI at −78 °C, and the resultant mixture (presumably containing $Cu(C{\equiv}C)_nSiMe_3$) was further treated with [(C^N^N)PtCl] to give [(C^N^N)Pt$(C{\equiv}C)_3SiMe_3$] (**12**) and [(C^N^N)Pt$(C{\equiv}C)_4SiMe_3$] (**13**) with a product yield of 56% and 4%, respectively. A similar protocol was previously used to prepare (η^5-C_5Me_5)(NO)(PPh_3)Re$(C{\equiv}C)_n$Cu intermediates.[26]

All complexes are air-stable and soluble in CH_2Cl_2, $CHCl_3$, acetone, THF, and DMSO, except **13**, **18**, and **22** which display low solubility in common organic solvents. All ^1H and ^{13}C (and ^{19}F where applicable) NMR spectra are well resolved. Thermal analysis by TGA in N_2 (see Supporting Information) show that the decomposition temperature is around 400 °C for **1**, **2**, **28**, and **29** and around 330 °C for **8**, **10**, and **11** (the residual decomposition product is composed of metallic platinum). This thermal stability is remarkable for σ-alkynylmetal complexes and especially for oligoynyl derivatives, i.e., the butadiynyls **8** and **11**.

Crystal Structures. Single crystals of **1**, **2**, **7**, **8**, and **10**−**12**, obtained from their DMSO solutions, were solved by X-ray crystallography (see Supporting Information for crystal data and selected bond lengths and angles; the structures of **2** and **8** were reported in our earlier communication[19]). In each structure, the Pt atom resides in a distorted square planar geometry that is comparable to those found for previously reported [(C^N^N)PtL]$^{n+}$ derivatives. The Pt−C(acetylide) distances range from 1.957(9) to 1.98(1) Å, which are similar to the values of 1.94 to 1.96 Å for [(tpy)PtC≡CPh](PF_6)[27] and [(α-diimine)Pt$(C{\equiv}CAr)_2$] complexes.[6a,7] For **1**, **2**, **7**, and **8**, the acetylenic units have alternating C≡C and C−C distances and deviate slightly from linear geometry, as indicated by the angles at the acetylenic carbon atoms (177 and 178° for **1**, 174 and 172° for **2**, 179 and 173° for **7**, and 175, 176, 177 and 177° for **8**, respectively). The dihedral angle between the acetylenic phenyl ring and the plane of the [(C^N^N)Pt] moiety for **1**, **2**, **7**, and **8** is 56, 7, 5 and 44°, respectively.

For the structures of **10**−**12**, the oligoyne moiety is systematically lengthened from trimethylsilyl-capped ethynyl to butadiynyl and hexatriynyl. As a direct consequence of this extension, the deviation of the acetylenic unit from linearity increases. Although each of the bond angles at the acetylenic carbon vertexes (172−178°) remains close to 180°, the accumulation of this effect for six angles in the crystal structure of **12** makes the hexatriynyl moiety appear like an arch. These curved structures have been previously observed in symmetrically and unsymmetrically endcapped oligoyne crystals and are presumably caused by crystal packing factors.[28] The Si−C(acetylide) distance also increases marginally from 1.800(8) Å for **10** and 1.827(8) Å for **11** to 1.89(4) Å for **12** with the extension of the oligoyne chain.

Interesting intermolecular interactions and conformations have been observed in these crystal lattices (Figures 1−3). For crystals **1**, **2**, **8**, and **10**−**12**, neighboring complex molecules are stacked into pairs in a head-to-tail fashion, with $\pi{-}\pi$ separations of ca. 3.5 Å. For crystal **7** (Figure 3), there are extensive C−H···F−C interactions[29] (with typical H···F distances in the 2.55−2.78 Å range) between the peripheral hydrogen atoms of the (C^N^N) ligand and the fluorine atoms of the neighboring pentafluorophenylacetylide moiety; these weak noncovalent contacts arrange the complex molecules into stacked sheets with interlayer distances of ca. 3.5 Å. For crystal **12** (Figure 2c), the intermolecular Pt−Pt contact of 3.466 Å between adjacent molecules is comparable to those reported for [$(tpy)_2Pt_2(\mu$-pz)]$(ClO_4)_3$ (3.432 Å; Hpz = pyrazole)[30] and related diphosphine-bridged derivatives.[16d]

Tuning of Spectroscopic Properties. To facilitate comparison, all absorption and emission spectra are recorded in CH_2-

(25) Rubin, Y.; Lin, S. S.; Knobler, C. B.; Anthony, J.; Boldi, A. M.; Diederich, F. *J. Am. Chem. Soc.* **1991**, *113*, 6943−6949.
(26) Weng, W.; Bartik, T.; Brady, M.; Bartik, B.; Ramsden, J. A.; Arif, A. M.; Gladysz, J. A. *J. Am. Chem. Soc.* **1995**, *117*, 11 922−11 931.
(27) Yam, V. W. W.; Tang, R. P. L.; Wong, K. M. C.; Cheung, K. K. *Organometallics* **2001**, *20*, 4476−4482.
(28) (a) Dembinski, R.; Bartik, T.; Bartik, B.; Jaeger, M.; Gladysz, J. A. *J. Am. Chem. Soc.* **2000**, *122*, 810−822. (b) Mohr, W.; Stahl, J.; Hampel, F.; Gladysz, J. A. *Inorg. Chem.* **2001**, *40*, 3263−3264. (c) Bruce, M. I.; Hall, B. C.; Kelly, B. D.; Low, P. J.; Skelton, B. W.; White, A. H. *J. Chem. Soc., Dalton Trans.* **1999**, 3719−3728. (d) Guillemot, M.; Toupet, L.; Lapinte, C. *Organometallics* **1998**, *17*, 1928−1930. (e) Sakurai, A.; Akita, M.; Moro-oka, Y. *Organometallics* **1999**, *18*, 3241−3244.
(29) Thalladi, V. R.; Weiss, H. C.; Bläser, D.; Boese, R.; Nangia, A.; Desiraju, G. R. *J. Am. Chem. Soc.* **1998**, *120*, 8702−8710.

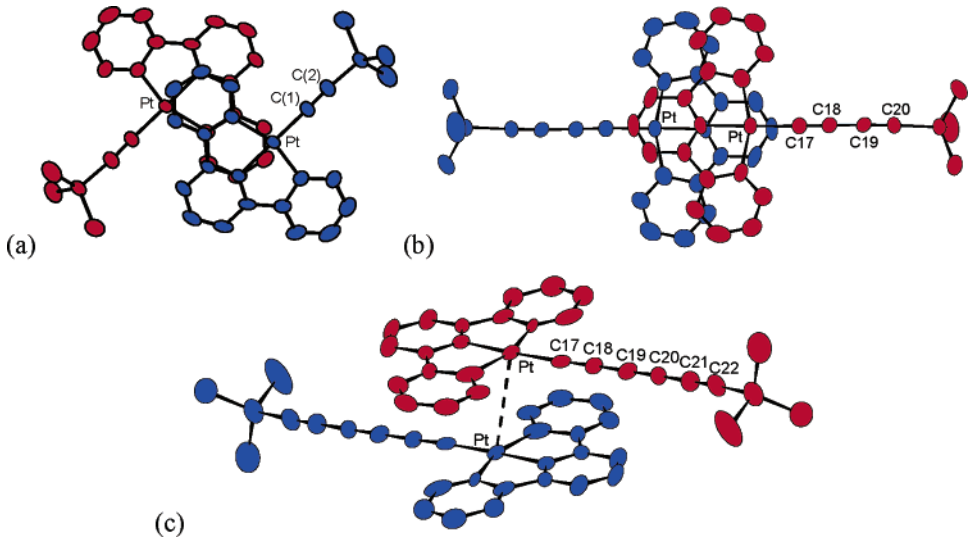

Figure 2. Crystal packing diagrams of **10** (a), **11** (b), and **12** (c), illustrating intermolecular contacts.

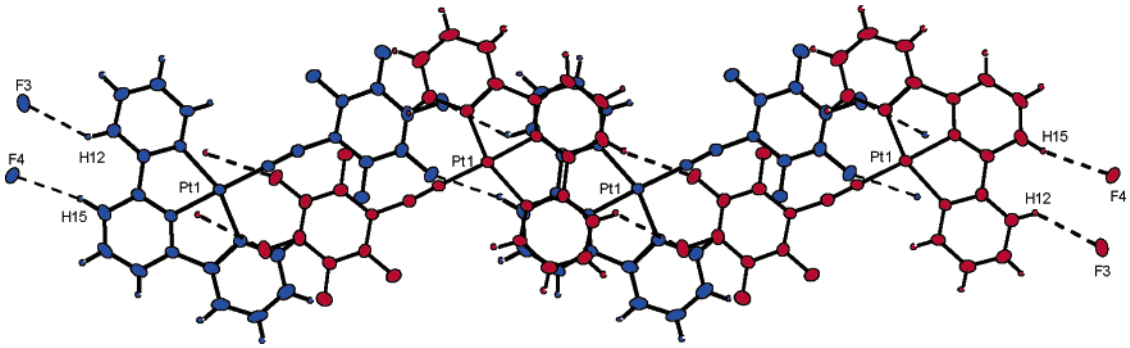

Figure 3. Crystal packing diagram of **7**, illustrating intermolecular contacts.

Cl_2 at 298 K and in alcoholic glass (CH_3OH/C_2H_5OH = 1/4) at 77 K except otherwise stated, and these spectroscopic data are summarized in Table 1. All complexes except **3**, **31**, and **32** are highly emissive in fluid solutions at 298 K with emission maxima in the 560−644 nm range and lifetimes in the microsecond regime. The solid-state emissions of these complexes vary from λ_{max} 564 to 715 nm but no distinct relationship is evident between molecular structures and emission energies.

(1) Variation of Arylacetylide Substituents. The electronic absorption spectra of **1**−**6** in CH_2Cl_2 solution at 298 K (see Supporting Information) show broad low-energy bands in the 410−470 nm range ($\epsilon \approx 5 \times 10^3$ dm^3 mol^{-1} cm^{-1}), which are red-shifted (and more intense) compared to those of [(C^N^N)PtL]$^+$ (L = pyridine, phosphines, etc., λ_{max} 380−420 nm, $\epsilon \leq 1.5 \times 10^3$ dm^3 mol^{-1} cm^{-1}; assigned as ^{1}MLCT transitions).[16d] These low-energy absorption peak maxima appear at 415 to 465 nm and systematically red-shift in accordance with the electron-donating ability of the para-substituent on the phenylacetylide ligand. The high-energy absorption bands of **1**−**5** located at λ_{max} 330−370 nm are attributed to intraligand (IL) charge-transfer transitions of the (C^N^N) ligand. For **6**, there is an additional intense absorption band at λ_{max} 375 nm ($\epsilon \approx 2.5 \times 10^4$ dm^3 mol^{-1} cm^{-1}), which is characteristic of the ^{1}IL-(4-nitrophenylacetylide) charge-transfer transition.[6b] Excitation of complexes **1**−**6** in fluid solution at room temperature results in long-lived (τ in μs scale) yellow to red luminescence (Table 1, Figure 4). The emission energies of the [(C^N^N)PtC≡CC$_6$H$_4$-4-R] series are red-shifted from the [(C^N^N)PtCl] precursor, in line with the absorption studies. The emission maxima in dichloromethane at 298 K varies from 630 nm for **3** to 560 nm for **6**, a range of 1980 cm^{-1}, and is affected by the para-substituent in the order (λ_{max}, nm): MeO > Me > F ≈ H ≈ Cl > NO_2. The radiative decay rate constants k_{nr} in CH_2Cl_2 solution at 298 K for these emissions are in the 10^4−10^5 s^{-1} range and the plot of ln k_{nr} against emission peak energy affords good linearity (Figure 4, inset), and is thus in agreement with the energy gap law. Complex **1** was chosen to examine the effect of solvent upon the low-energy absorption and emission spectra (see Supporting Information). When the polarity of the solvent decreases from ethanol and acetonitrile to CH_2Cl_2 and benzene, the low-energy broad absorption band red-shifts in energy, and in the cases of CH_2Cl_2 and benzene, two distinguishable absorption peak maxima are observed. In addition, the emission λ_{max} slightly red-shifts from 580 to 585 nm, while the lifetime and quantum yield changes from 0.3 to 0.6 μs and 0.03 to 0.07, respectively.

Except for **3**, the emission quantum yields of these complexes in CH_2Cl_2 are comparable to that of [Ru(bpy)$_3$]$^{2+}$ (bpy = 2,2′-bipyridine) salts (0.062 in acetonitrile). As previously observed for related Pt(II) lumophores,[6a,16] the self-quenching constants k_q of the emissions of **1**−**6** in CH_2Cl_2 range from 3.1×10^9 s^{-1} dm^{-1} mol^{-1} for **6** to 5.7×10^9 s^{-1} dm^{-1} mol^{-1} for **2** at room temperature (Table 1). The solid-state emissions of **1**−**6** at 298 K are broad with λ_{max} in the 590−720 nm range. However, a

(30) Bailey, J. A.; Miskowski, V. M.; Gray, H. B. *Inorg. Chem.* **1993**, *32*, 369−370.

Table 1. Spectroscopic Data

complex	absorption:[a] λ_{max}/nm (ϵ/$\times 10^3$ dm^3 mol^{-1} cm^{-1})	emission in fluid solution:[b] λ_{max}/nm (τ/μs; ϕ); k_q/10^9 s^{-1} dm^{-1} mol^{-1}; k_{nr}/10^6 s^{-1}	emission in alcoholic glass:[c] λ_{max}/nm (τ/μs)	solid-state emission (298 K): λ_{max}/nm (τ/μs)	solid-state emission (77 K): λ_{max}/nm (τ/μs)
[(C^N^N)PtC≡CC_6H_5] (**1**)	229 (29.7), 281 (38.3), 335 (14.0), 366 (9.98), 434 (5.18), 455 (4.94)	582 (0.4; 0.04); 4.7; 2.5	540, 574 (7.8)	592, 630 (sh) (0.5)	593, 639 (1.5)
[(C^N^N)PtC≡CC_6H_4-4-CH_3] (**2**)	245 (39.4), 281 (54.6), 335 (18.0), 366 (11.4), 440 (5.09), 460 (4.95)	600 (0.2; 0.02); 5.7; 5.8	534, 575 (7.8)	590, 615 (sh) (≤ 0.1)	589, 620 (0.6)
[(C^N^N)PtC≡CC_6H_4-4-OCH_3] (**3**)	245 (27.6), 280 (34.7), 335 (13.4), 366 (8.51), 440 (4.20), 465 (4.22)	630 (≤ 0.1; ≤ 10^{-3})	564 (8.8)	720 (≤ 0.1)	710 (≤ 0.1)
[(C^N^N)PtC≡CC_6H_4-4-Cl] (**4**)	230 (43.8), 283 (65.9), 334 (23.3), 365 (15.5), 432 (8.67), 455 (8.31)	578 (0.5; 0.08); 4.9; 1.7	529, 565 (8.2)	705 (≤ 0.1)	710 (0.9)
[(C^N^N)PtC≡CC_6H_4-4-F] (**5**)	247 (26.5), 266 (31.4), 279 (34.6), 334 (13.7), 368 (8.97), 433 (4.88), 453 (4.76)	585 (0.3; 0.03); 4.0; 2.4	542, 580 (7.1)	nonemissive	810 (≤ 0.1)
[(C^N^N)PtC≡CC_6H_4-4-NO_2] (**6**)	237 (39.1), 281 (27.9), 338 (19.8), 375 (24.6), 415 (12.9)	560 (0.9; 0.08); 3.1; 1.0	537, 572 (7.9)	616, 650 (sh) (0.4)	610, 650 (sh) (1.4)
[(C^N^N)PtC≡CC_6F_5] (**7**)	240 (28.2), 283 (38.7), 362 (10.4), 334 (15.2), 436 (5.46), 421 (5.45)	560 (0.6; 0.06)	531, 575 (5.9)	627 (≤ 0.1)	586, 620 (sh) (1.5)
[(C^N^N)Pt(C≡C)$_2C_6H_5$] (**8**)	231 (32.0), 281 (24.0), 316 (18.7), 366 (7.79), 430 (4.97)	571 (1.0; 0.08)	535, 572 (9.7)	647 (≤ 0.1)	568, 646 (≤ 0.1)
[(C^N^N)PtC≡C$C(CH_3)_3$] (**9**)	281 (25.0), 335 (13.9), 372 (7.40), 436 (3.69), 460 (3.40)	584 (0.4; 0.04)	540, 578 (8.0)	598 (0.31), 640 (sh)	585, 630 (2.2)
[(C^N^N)PtC≡C$Si(CH_3)_3$] (**10**)	242 (36.3), 263 (29.4), 281 (35.0), 334 (19.7), 366 (11.8), 427 (5.49), 450 (4.02)	570 (0.3; 0.04); 2.8; 3.1	531, 568 (7.7)	578, 615 (sh) (0.2)	575, 625 (1.1)
[(C^N^N)Pt(C≡C)$_2$$Si(CH_3)_3$] (**11**)	230 (48.0), 244 (4.39), 280 (30.4), 336 (17.5), 366 (10.8), 426 (6.40)	561 (0.2; 0.03)	532, 570 (7.0)	705 (0.3)	588 (2.1), 717 (1.2)
[(C^N^N)Pt(C≡C)$_3$$Si(CH_3)_3$] (**12**)	246 (65.2), 260 (75.0), 336 (17.2), 368 (10.8), 431 (8.87)	557 (0.8; 0.07)	530, 567 (10.2)	688 (0.7)	709 (1.6)
[(C^N^N)Pt(C≡C)$_4$$Si(CH_3)_3$] (**13**)	234 (37.3), 282 (82.8), 337 (17.4), 364 (11.8), 415 (6.34), 445 (8.61)	589, 671 (2.7; 0.01)	584, 667 (11.5)	n. d.	n. d.
[4-Ph(C^N^N)PtC≡CC_6H_5] (**14**)	229 (36.8), 285 (54.7), 337 (18.3), 370 (12.0), 441 (7.54), 462 (sh, 6.85)	597 (0.8; 0.07)	539, 580 (sh) (14)	613 (0.4)	601, 645 (sh) (3.1)
[4-(4-$CH_3C_6H_4$) (C^N^N)PtC≡CC_6H_5] (**15**)	230 (37.1), 284 (49.2), 332 (sh, 19.0), 370 (12.4), 442 (8.29), 460 (sh, 8.14)	597 (0.8; 0.09)	550, 590 (sh) (13.6)	593 (0.5)	584, 630 (4.7)
[4-(4-$CH_3OC_6H_4$) (C^N^N)PtC≡CC_6H_5] (**16**)	229 (44.2), 282 (51.7), 331 (32.1), 366 (sh, 16.4), 441 (9.94), 460 (sh, 9.18)	594 (1.0; 0.09)	544, 580 (sh) (14)	595 (0.2)	587, 634 (5.2)
[4-(4-ClC_6H_4) (C^N^N)PtC≡CC_6H_5] (**17**)	230 (38.2), 287 (53.0), 339 (17.9), 373 (12.2), 446 (8.13), 465 (sh, 7.89)	603 (0.7; 0.08)	547, 580 (sh) (12.7)	590 (≤ 0.1)	588, 635 (2.2)
[4-(4-$NO_2C_6H_4$) (C^N^N)PtC≡CC_6H_5] (**18**)	244 (39.9), 291 (54.4), 339 (25.3), 365 (sh, 16.4), 446 (8.41)	592 (0.5; 0.10)	558, 597 (15.5)	615, 710 (sh) (≤ 0.1)	604, 710 (sh) (≤ 0.1)
[4,4′-^{t}Bu_2(C^N^N) PtC≡CC_6H_5] (**19**)	247 (30.2), 283 (39.8), 330 (15.2), 360 (9.52), 426 (5.95), 432 (5.93)	571 (0.8; 0.05)	513, 550 (7.0)	543, 570, 610 (sh) (0.6)	549, 580 (8.9)
[4,4′-^{t}Bu_2(C^N^N) PtC≡CC_6F_5] (**20**)	239 (31.5), 281 (40.1), 329 (16.8), 357 (11.2), 413 (6.33), 439 (6.38)	550 (0.9; 0.07)	510, 546 (5.5); 715 (2.0)	563, 588, 640 (sh) (0.9)	545, 585 (5.0)
[4,4′-^{t}Bu_2(C^N^N)PtC≡C-pyrenyl-1] (**21**)	236 (64.8), 283 (45.6), 293 (46.5), 330 (18.0), 368 (30.9), 382 (30.2), 399 (24.8), 457 (broad, 8.6), 505 (sh, 4.2)	664, 723 (21; 0.01)	653 (114), 669, 710, 727	669 (weak)	669 (0.8), 687, 704, 717, 740,
[EtO_2C(C^N^N)PtC≡CC_6H_5] (**22**)	256 (36.6), 283 (42.4), 347 (15.7), 376 (10.8), 458 (5.89), 484 (5.79)	622 (0.3; 0.03)	568 (9.1)	749 (≤ 0.1)	590 (1.0), 642
[EtO_2C(C^N^N)PtC≡CC_6F_5] (**23**)	252 (32.5), 285 (46.6), 347 (17.9), 373 (12.8), 441 (6.98), 463 (7.99)	593 (1.6; 0.08)	558 (7.4), 599	601 (0.6)	591 (1.8), 642
[5″-CH_3(C^N^N)PtC≡CC_6H_5] (**24**)	228 (30.4), 251 (29.0), 282 (39.0), 337 (14.1), 367 (8.62), 437 (5.10), 460 (sh, 4.83)	590 (0.4; 0.02)	542 (6.1), 585	601, 654 (sh) (≤ 0.1)	596, 645 (2.0)
[4″-CH_3(C^N^N)PtC≡CC_6H_5] (**25**)	229 (29.8), 282 (40.5), 338 (13.7), 369 (10.5), 436 (4.61), 455 (sh, 4.32)	579 (0.4; 0.03)	534 (6.6), 578	604, 653 (≤ 0.1), 705	563, 603 (≤ 0.1), 649

Table 1 (Continued)

complex	absorption:[a] λ_{max}/nm (ϵ/× 10^3 dm^3 mol^{-1} cm^{-1})	emission in fluid solution:[b] λ_{max}/nm (τ/μs; ϕ); k_q/10^9 s^{-1} dm^{-1} mol^{-1}; k_{nr}/10^6 s^{-1}	emission in alcoholic glass:[c] λ_{max}/nm (τ/μs)	solid-state emission (298 K): λ_{max}/nm (τ/μs)	solid-state emission (77 K): λ_{max}/nm (τ/μs)
[4″-CF_3(C^N^N)PtC≡CC_6H_5] (**26**)	229 (31.4), 268 (34.6), 183 (38.3), 329 (16.7), 365 (sh, 8.30), 435 (5.55), 454 (5.65)	590 (0.5; 0.05)	519 (9.9), 542	nonemissive	nonemissive
[2″,4″-F_2(C^N^N)PtC≡CC_6H_5] (**27**)	229 (29.4), 253 (33.6), 280 (40.8), 332 (13.3), 355 (sh, 9.61), 441 (4.76)	582 (0.7; 0.07)	515 (18.9)	564, 603 (0.4)	559, 608, 654 (4.2)
[(S^N^N)PtC≡CC_6H_5] (**28**)	256 (24.7), 280 (32.6), 321 (19.1), 371 (14.9), 436 (4.97), 460 (4.49)	615, 660 (sh) (1.0; 0.05)	595, 644 (8.7)	630, 660 (0.3)	628, 684 (1.5)
[(S^N^N)PtC≡CC_6H_4-4-CH_3] (**29**)	259 (26.9), 279 (35.0), 323 (19.2), 373 (15.2), 442 (5.01), 465 (4.80)	616, 660 (sh) (0.9; 0.04)	595, 646 (8.1)	625, 655 (0.5)	624, 678 (1.5)
[(S^N^N)PtC≡CC_6F_5] (**30**)	229 (22.1), 252 (18.8), 282 (28.0), 314 (1.81), 369 (13.9), 421 (4.90), 437 (4.88)	616, 660 (sh) (1.1, 0.04)	594 (8.9), 646, 713 (3.1)	~630, 664 (0.4)[d]	627 (1.1), 672
[(O^N^N)PtC≡CC_6H_5] (**31**)	233 (31.9), 281 (40.4), 310 (sh, 22.3), 364 (17.0), 434 (5.80), 457 (5.34)	~640 (≤ 0.1; ≤ 10^{-3})[d]	613, 664 (4.1)	715 (≤ 0.1)	755 (≤ 0.1)
[(O^N^N)PtC≡CC_6H_4-4-CH_3] (**32**)	229 (33.0), 278 (39.7), 367 (14.6), 432 (5.91), 465 (sh, 5.47)	~640 (≤ 0.1; ≤ 10^{-3})[d]	610, 664 (4.3)	~720 (≤ 0.1)[d]	629 (0.15); 757 (≤ 0.1)
[(O^N^N)PtC≡CC_6F_5] (**33**)	230 (32.2), 283 (40.8), 376 (15.4), 417 (6.72), 432 (sh, 6.40)	644, 680 (sh) (0.9, 0.02)	610, 664 (4.8)	nonemissive	nonemissive

[a] Measured in CH_2Cl_2 solution at 298 K. [b] Measured in degassed CH_2Cl_2 solution at 298 K (concentrations ~1 × 10^{-5} mol dm^{-3}). [c] Measured in CH_3OH/C_2H_5OH = 1/4 at 77 K. [d] Very weak (n.d. = not determined).

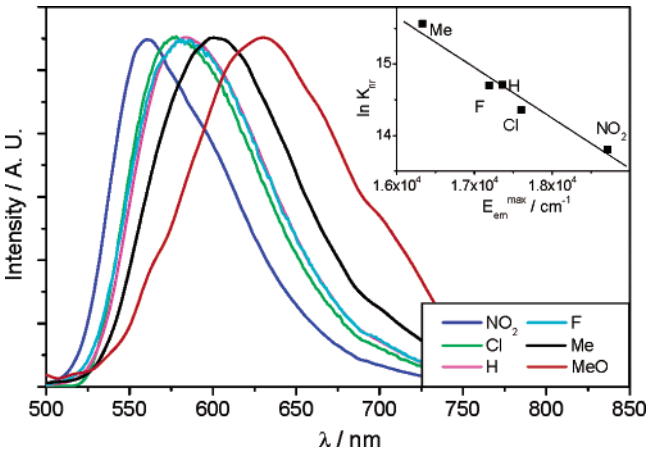

Figure 4. Normalized emission spectra of complexes **1**−**6** in CH_2Cl_2 solution at 298 K (λ_{ex} = 350 nm). Inset: plot of ln k_{nr} versus emission maximum (legends indicate 4-arylacetylide substituents in the [(C^N^N)-PtC≡CC_6H_4-4-R] series).

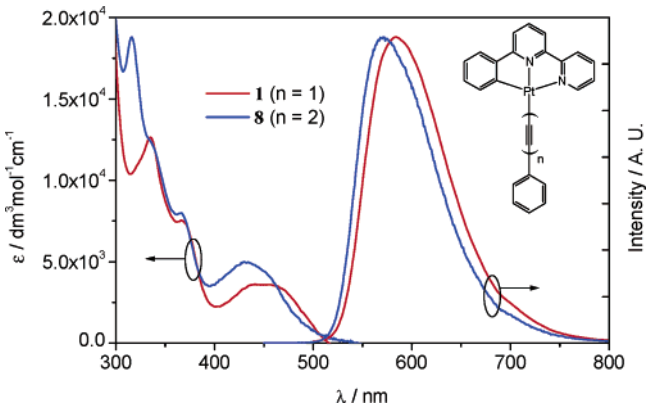

Figure 5. UV-vis absorption and normalized emission (λ_{ex} = 350 nm) spectra of complexes **1** and **8** in CH_2Cl_2 solution at 298 K.

correlation between the solid-state emission and substituents on the arylacetylide ligand is not apparent.

(2) Extension of Oligoyne Ligand. The effects of the π-conjugated length of the oligoyne ligands upon the emission of [(C^N^N)Pt−$(C≡C)_n$−R] have been examined. When the alkynyl ligand is extended from phenyl-capped ethynyl (**1**) to butadiynyl (**8**), the lowest absorption peak maximum of the broad MLCT transition band in CH_2Cl_2 solution blue-shifts from ~460 to ~430 nm, while the corresponding emission λ_{max} partially blue-shifts by ca. 330 cm^{-1} from 582 to 571 nm (Figure 5). In the 77 K alcoholic glass spectra, the emission λ_{max} (λ_{0-0}) blue-shifts by only ca. 170 cm^{-1} from 540 nm for **1** to 535 nm for **8** (see Supporting Information for spectra).

From **10** to **12**, the alkynyl ligand is homologously lengthened from trimethylsilyl-capped ethynyl to hexatriynyl. The low-energy bands beyond 400 nm in the absorption spectra of **10**−**12** in CH_2Cl_2 solutions at 298 K are similar and poorly resolved (see Supporting Information for spectra). The emission quantum yields and lifetimes of these three complexes are comparable. The emission energies in CH_2Cl_2 solution at 298 K (Figure 6) decrease in the order: triynyl (λ_{max} 557 nm) > diynyl (λ_{max} 561 nm) > monoynyl (λ_{max} 570 nm), but the differences are minor, as are those found in glassy alcoholic solutions at 77 K.

Stark changes in the absorption and emission spectra are observed when the trimethylsilyl-capped oligoyne ligand is further extended to octatetraynyl (**13**), the next homologue. In the absorption spectrum of **13** in CH_2Cl_2 solution at 298 K (see Supporting Information for spectra), the low-energy bands are well resolved into two distinct peak maxima at 411 and 444 nm. Saliently, **13** exhibits highly structured, narrow-bandwidth emission at 298 K, with peak maxima at λ_{max} 589 and 671 nm (Figure 6) and emission lifetime of 2.7 μs (complex concentration ≈ 1.5 × 10^{-5} mol dm^{-3}). The vibronic progression of ca. 2100 cm^{-1} signifies that the −$(C≡C)_4$− unit is involved in the

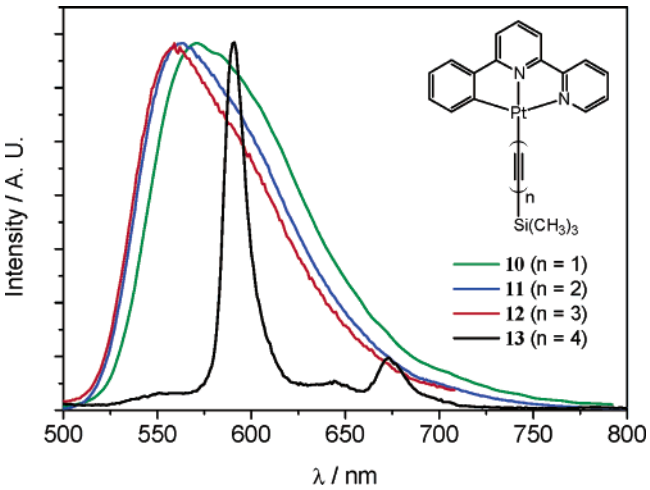

Figure 6. Emission spectra of **10**−**13** in CH_2Cl_2 solution at 298 K (λ_{ex} = 350 nm).

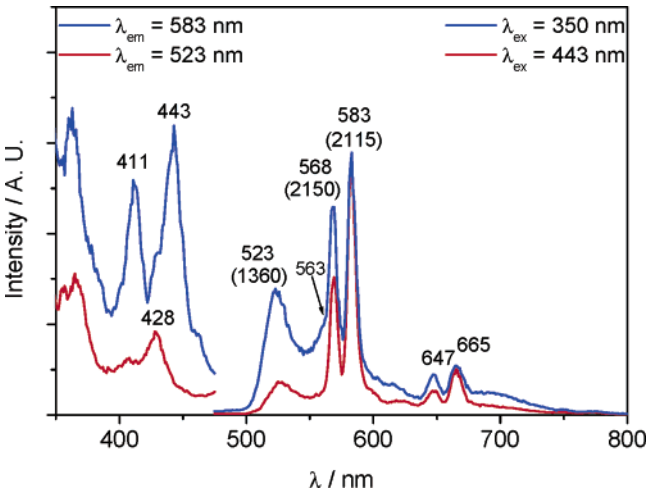

Figure 7. Site-selective emission [vibronic progression (cm^{-1}) in parentheses] and excitation spectra of **13** in alcoholic glassy solution at 77 K (concentration ~1 × 10^{-5} mol dm^{-3}).

electronic transition (see section on ethynylpyrene complex **21**). The emission maximum slightly red-shifts from 588 to 589, 591 and 594 nm when the solvent polarity decreases from ethanol to CH_2Cl_2, THF and toluene, respectively. This emission is similar in energy and shape to the acetylenic $^3\pi\pi^*$ emission of $[(Cy_3P)Au(C{\equiv}C)_4Au(PCy_3)]$[31] ($\lambda_{0-0}$ 574 nm with vibronic progression of 2120 cm^{-1} in CH_2Cl_2 at 298 K), except for a minor red-shift of ~440 cm^{-1}. In alcoholic glassy solution at 77 K, complex **13** exhibits multiple and site-selective emissions. Structured emission is observed upon excitation at 350 nm (Figure 7), which resembles overlapping of three emissions with different origins, namely: (1) λ_{0-0} 523 nm with vibronic progression of ca. 1360 cm^{-1}, (2) λ_{0-0} 568 nm with vibronic progression of 2150 cm^{-1}, and (3) λ_{0-0} 584 nm with vibronic progression of 2115 cm^{-1}. Upon excitation into a lower-energy band (443 nm), the emission energies do not alter but the relative intensity of the 523 nm band decreases. Moreover, the excitation spectra monitored at λ_{em} 583 and 523 nm are different in the 400−500 nm spectral range; two peak maxima at 411 and 433 nm were recorded for the former, while a band at λ_{max} 428 nm was detected for the latter.

(31) Lu, W.; Xiang, H. F.; Zhu, N.; Che, C. M. *Organometallics* **2002**, *21*, 2343−2346.

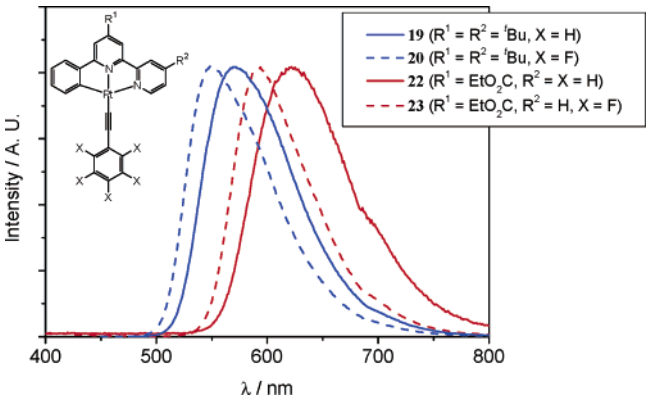

Figure 8. Emission spectra of **19**, **20**, **22**, and **23** in CH_2Cl_2 solution at 298 K (λ_{ex} = 350 nm, concentration ~1 × 10^{-5} mol dm^{-3}).

Additionally, complex **9** with a *tert*-butylacetylide ligand, which is the C-congener of the trimethylsilyl acetylide **10**, was prepared. The lower-energy absorption band of **9** in CH_2Cl_2 solution is slightly red-shifted from that of **10** by ca. 650 cm^{-1}. Similarly, **9** exhibits intense orange emission with λ_{max} at 586 nm in CH_2Cl_2 solution, which is red-shifted from the emission displayed by **10** (λ_{max} 570 nm). When the polarity of the solvent decreases from ethanol and acetonitrile to CH_2Cl_2 and benzene (see Supporting Information), red shifts are detected for both the low-energy absorption band maximum (from 422 to 479 nm) and the emission λ_{max} (from 579 to 587 nm), while the lifetime and quantum yield changes from 0.3 to 0.4 μs and 0.02 to 0.04, respectively.

(3) Derivatization of Tridentate Cyclometalating Ligand. Modifications of the substituents on the (C^N^N) ligand have been undertaken in order to facilitate the fine-tuning of the emission energy for the [(C^N^N)PtC≡C−R] complexes. Attachment of a *para*-substituted aryl ring at the 4-position of the (C^N^N) ligand afforded Pt(II) complexes that are more robust but less soluble in common organic solvents. In CH_2Cl_2 solution at 298 K, the low-energy absorption band of **18**, bearing an electron-withdrawing nitro group at the said para-position, contains a distinct peak maximum at 446 nm. This transition is blue-shifted from that for **14**−**17**, which occurs as a broad band in the 400−550 nm range (see Supporting Information for spectra). However, **14**−**18** exhibit similar orange-red emissions with λ_{max} around 595 nm in CH_2Cl_2 solution at 298 K, and the emission energies and quantum yields are comparable to those for the parent complex [(C^N^N)PtC≡CPh] (**1**). This implies that the impact of the 4-aryl ring is relatively small with regards to the emission properties of this class of emitters.

The introduction of two *tert*-butyl groups to the bipyridine moiety of the (C^N^N) ligand affects the emission properties of **19** and **20** (Figure 8). The electron-donating nature of the *tert*-butyl groups leads to blue-shifted emissions for **19** (λ_{max} 571 nm) and **20** (λ_{max} 550 nm) compared to the parent complexes **1** (λ_{max} 582 nm) and **7** (λ_{max} 560 nm), respectively, in CH_2Cl_2 solution at 298 K. The bulky *tert*-butyl groups presumably also minimize solid-state intermolecular interactions between neighboring [(C^N^N)Pt] planes. Accordingly, the bright yellow color of crystalline **19** and **20**, which is in contrast to the deep red/brown color of the [(C^N^N)PtC≡CC_6H_4-4-R] series in the solid state, is likely to be a consequence of blue-

shifted electronic transitions due to the lack of intermolecular interactions. Conversely, the electron-withdrawing ethoxycarbonyl group on the 4-position of the (C^N^N) ligand dramatically red-shifts the emission maximum for **22** (620 nm) and **23** (593 nm) compared to **1** (582 nm) and **7** (560 nm), respectively, in CH_2Cl_2 solution (Figure 8).

Incorporation of methyl, CF_3 and F substituents onto the phenyl ring of the (C^N^N) ligand result in relatively small differences in the low-energy absorption (see Supporting Information for spectra) and emission properties of the complexes. Hence, complexes **24**−**27** exhibit intense orange emissions ($\lambda_{max} \approx 585$ nm) with comparable quantum yields and lifetimes in CH_2Cl_2 solution at 298 K (Table 1).

With the development of red emitters as a clear objective, the [(S^N^N)PtC≡CR] (**28**−**30**) and [(O^N^N)PtC≡CR] (**31**−**33**) (R = Ph, C_6H_4-4-Me, and C_6F_5 respectively) complexes containing the thienyl or furyl moiety as cyclometalating carbon donor, respectively, were synthesized. The absorptions in the 300−400 nm range in the absorption spectra of **28**−**33** (see Supporting Information for spectra) are assigned to ^{1}IL transitions of the (S^N^N) and (O^N^N) ligand, respectively, and they are red-shifted from those of the corresponding (C^N^N) complexes. The low-energy absorption for **28**−**33** is comparable to those of the (C^N^N) congeners **1**, **2**, and **7**, respectively, but the mild tendency to red-shift from (C^N^N)- to (S^N^N)- and (O^N^N)-based lumophores is discernible. For example, the edge of the lower-energy absorption band partially red-shifts from **1** (∼460 nm) to **28** (∼470 nm) and **31** (∼475 nm). Upon excitation with UV light, **28**−**30** gives intense red emission in CH_2Cl_2 at λ_{max} 616 nm (shoulder 660 nm), irrespective of the arylacetylide substituents, and the spectral profile of this emission is similar to that of [Pt(S^N)$_2$] (HS^N = 2-(2-thienyl)-pyridine)[32] except that the emission maximum is red-shifted by 860 cm^{-1}. In the solid state, the emission shows well-resolved vibronic structure with a progression of ∼1300 cm^{-1} and slightly red-shifts to λ_{max} 630 nm, while in alcoholic glassy solutions, the emission maximum blue-shifts to 595 nm. In glassy alcoholic solution at 77 K, **31**−**33** emits strongly at λ_{max} 610 nm with a shoulder at 664 nm, again irrespective of the substituents on the arylacetylide ligand. Complexes **31** and **32** are weakly emissive in fluid solutions, while **33** bearing a pentafluorophenylacetylide ligand is emissive [λ_{max} 644 (shoulder 680) nm] in CH_2Cl_2 solution at 298 K. The effects of solvent upon the spectroscopic properties of **28** and **33** have been examined (see Supporting Information for spectra). When the solvent changes from ethanol to acetonitrile, CH_2Cl_2 and benzene, the low-energy broad absorption band splits into two distinct peaks and the edge of this absorption manifold red-shifts from ca. 450 to 500 nm for **28** and from ca. 420 to 450 nm for **33**. Nevertheless, the emission maximum only undergoes a slight red-shift from 608 to 619 nm for **28** and from 634 to 647 nm for **33**, and the lifetime (quantum yield) remains relatively constant at ca. 1.0 μs (0.04) for **28** and ca. 0.4 μs (0.02) for **33**.

For comparison, the emission spectra of **1**, **28**, and **31** [(C≡CPh) complexes] in alcoholic glass at 77 K and **7**, **30**, and **33** [(C≡CC_6F_5) complexes] in CH_2Cl_2 solution at 298 K are shown in Figures 9 and 10, respectively. For the same arylacetylide ligand, the emission maximum substantially red-shifts when the

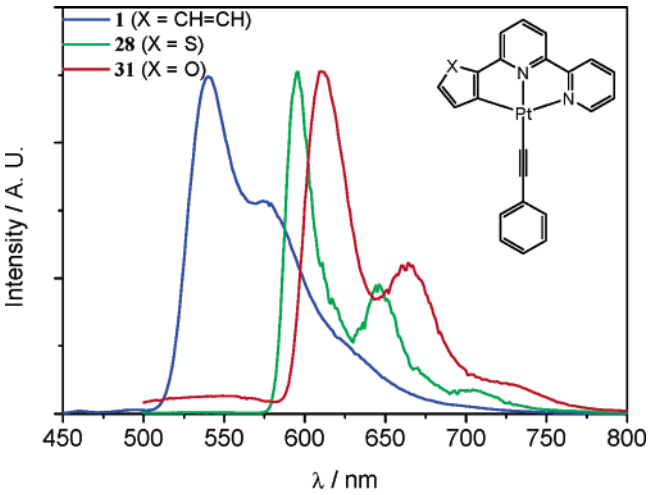

Figure 9. Emission spectra of **1**, **28** and **31** in alcoholic glass at 77 K (λ_{ex} = 350 nm, concentration ∼1 × 10^{-5} mol dm^{-3}).

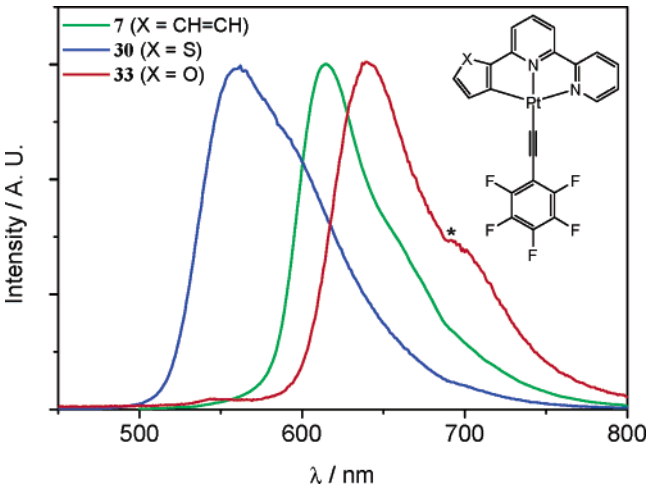

Figure 10. Emission spectra of **7**, **30** and **33** in CH_2Cl_2 solution at 298 K (λ_{ex} = 350 nm, concentration ∼1 × 10^{-5} mol dm^{-3}, * denotes instrumental artifact).

cyclometalating ligand is modified from (C^N^N) to (S^N^N) and (O^N^N). The Huang−Rhys ratios ($S = I_{1-0}/I_{0-0}$, estimated using relative peak intensities) of the emissions recorded in glassy solutions appear to decrease in the sequence of **1** (ca. 0.6) > **31** (ca. 0.5) > **28** (ca. 0.4), and similar values were also recorded in fluid solutions. While **1** is a yellow light emitter, the excited-state properties of **28**−**30** and **33** have been adjusted to yield orange-red and saturated red emissions, respectively.

(4) Red-Shifted and Narrow-Width Emission from [4,4′-^{t}Bu$_2$-(C^N^N)PtC≡Cpyrenyl-1] (21). When 1-ethynylpyrene, which has a low-lying triplet excited state,[33] was employed as auxiliary acetylide ligand in complex **21**, a low-energy and narrow-bandwidth emission (Figure 11) was observed at λ_{0-0} (λ_{max}) 664 nm with major vibronic progression, lifetime and quantum yield of 1230 cm^{-1}, 20.8 μs and 0.01, respectively, in CH_2Cl_2 solution at 298 K. This emission is similar in energy to that (λ_{max} ca. 660 nm) observed for [(^{t}Bu$_2$bpy)Pt(C≡Cpyrenyl-1)$_2$] (^{t}Bu$_2$bpy = 4,4′-bis-*tert*-butyl-2,2-bipyridine)[6e] but slightly lower than the $^3\pi\pi^*$ emission recorded for [(Cy_3P)AuC≡Cpyrenyl-1] (λ_{0-0} 654 nm in the solid-state at 298 K, see

(32) Maestri, M.; Sandrini, D.; Balzani, V.; Chassot, L.; Jolliet, P.; von Zelewsky, A. *Chem. Phys. Lett.* **1985**, *122*, 375−379.

(33) McGlynn, S. P.; Azumi, T.; Kinoshita, M. *Molecular Spectroscopy of the Triplet State*; Prentice Hall: Englewood NJ, 1969.

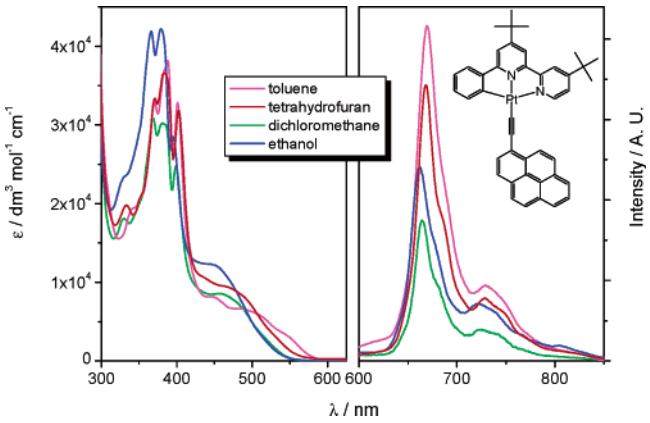

Figure 11. Absorption and emission spectra of **21** in various solvents at 298 K (λ_{ex} = 350 nm, concentration ~1 × 10^{-5} mol dm^{-3}).

Table 2. Electrochemical Data[a] of Selected Complexes

complex	reduction $E^{1/2}$ (V)[b]	anodic peak E_{pa} (V)[b]
[(C^N^N)PtC≡CPh] (**1**)	−1.81	0.04
[(C^N^N)PtC≡CC_6H_4-4-CH_3] (**2**)	−1.77	0.01
[(C^N^N)PtC≡CC_6H_4-4-OCH_3] (**3**)	−1.84	0.08
[(C^N^N)PtC≡CC_6H_4-4-NO_2] (**6**)	−1.61	0.12
[(C^N^N)PtC≡CC_6F_5] (**7**)	−1.78	0.09
[(C^N^N)PtC≡$CC(CH_3)_3$] (**9**)	−1.87	0.29
[(C^N^N)PtC≡$CSi(CH_3)_3$] (**10**)	−1.82	0.47
[(C^N^N)Pt(C≡C)$_2$$Si(CH_3)_3$] (**11**)	−1.77	0.28
[(C^N^N)Pt(C≡C)$_3$$Si(CH_3)_3$] (**12**)	−1.76	0.22
[(C^N^N)Pt(C≡C)$_4$$Si(CH_3)_3$] (**13**)	−1.70	*c*
[4,4′-^{t}Bu_2(C^N^N)PtC≡CPh] (**19**)	−1.93	0.29
[EtO_2C(C^N^N)PtC≡CPh] (**22**)	−1.60	0.05
[(S^N^N)PtC≡CC_6F_5] (**30**)	−1.80	0.12
[(O^N^N)PtC≡CC_6F_5] (**33**)	−1.77	0.18

[a] Determined in CH_2Cl_2 at 298 K with 0.1 M ^{n}Bu_4NPF_6 as supporting electrolyte; scanning rate: 50 mV s^{-1}. [b] Value versus $E^{1/2}$ ($Cp_2Fe^{+/0}$) [0.11−0.13 V versus Ag/$AgNO_3$ (0.1 M in CH_3CN) reference electrode]. [c] Beyond the spectral window of CH_2Cl_2 solvent.

Supporting Information for spectra) by ca. 230 cm^{-1}. The emission maximum slightly red-shifts from 662 to 664, 668 and 669 nm when the solvent polarity decreases from ethanol to CH_2Cl_2, THF and toluene, respectively. In contrast, the low-energy band in the absorption spectrum of **21** exhibits more prominent solvatochromism, thus the low-energy shoulder shifts from *ca.* 450, to 475, 520 and 550 nm when the solvent polarity decreases from ethanol to CH_2Cl_2, THF and toluene, respectively (left of Figure 11).

Time-Resolved Absorption Spectroscopy. The triplet excited-state absorption spectra of **1** and **28** in CH_3CN solution have been recorded (see Supporting Information for spectra). In both cases, the decay of the absorption signals corresponds to the emission lifetime, indicating that the absorption originated from the emissive excited state. The salient features in these spectra are, for **1**, strong bleaching in the near UV region (400−460 nm), absorption in the 460−520 nm range and intense luminescence bleaching in the 520−750 nm range, and for **28**, strong absorption in the 380−570 nm range (λ_{max} ca. 400, 490 and 530 nm) and intense luminescence bleaching in the 570−750 nm range.

Cyclic Voltammetry. The electrochemical data of several Pt(II) complexes are summarized in Table 2. In general, the cyclic voltammograms in CH_2Cl_2 solutions at 298 K exhibit one reversible reduction couple with $E^{1/2}$ in the range −1.60 to −1.93 V versus $Cp_2Fe^{+/0}$; this couple presumably corresponds to the one-electron reduction of the (C^N^N) ligand. Substitution at the (C^N^N) ligand exerts a more substantial effect upon the $E^{1/2}$ value than at the arylacetylide ligand. The electron-withdrawing ethoxycarbonyl group in **22** shifts the first reduction wave to −1.60 V, while this reduction occurs at −1.93 V for **19** which bears two electron-donating *tert*-butyl groups. Complex **6**, with a nitro group on the *para*-position of the arylacetylide ligand, shows a higher $E^{1/2}$ value of −1.61 V for the reduction of the (C^N^N) moiety. The conjugation length of the oligoynyl ligand does not significantly affect the (C^N^N) reduction. The (C^N^N), (S^N^N), and (O^N^N) derivatives containing the pentafluorophenylacetylide ligand show comparable reduction waves.

Except **13**, all complexes show an irreversible oxidation wave at 0.01−0.47 V versus $Cp_2Fe^{+/0}$ (0.41−0.87 V versus NHE). Complex **10**, which features the shortest conjugation length at the acetylide moiety, exhibits the most positive oxidation peak potential of 0.47 V. The ethoxycarbonyl group in **22** shifts the first oxidation wave to 0.05 V while this oxidation occurs at 0.29 V for the bis(*tert*-butyl)-substituted **19**.

Table 3. Electroluminescence Data

complex	EL λ_{max}[a]/nm (CIE coordinates[a] [x, y])	turn-on voltage/V	doping ratio (%)	maximum luminance/ cd m^{-2}	maximum efficiency/ cd A^{-1}	maximum η_{ext}/%
1	564	3.6	2[b]	9900[e]	4.2[h]	1.6
	(0.480, 0.484)		4	7800[d]	2.4[h]	0.9
2	580	4.2	4	3900[e]	1.4[g]	0.6
	(0.508, 0.466)		6	2100[e]	0.6[g]	0.3
7	548	4.5	2[b]	5600[f]	1.5[h]	0.3
	(0.440, 0.507)		4	9800[e]	3.2[g]	1.1
9	567	4.5	5	5800[c]	1.4[g]	0.6
	(0.480, 0.469)					
20	545	4.3	4	5500[d]	1.9[g]	0.1
	(0.419, 0.526)		6	2090[d]	0.5[i]	0.2
28	608, 656	4.5	2[b]	2000[e]	0.7[h]	0.6
	(0.549, 0.330)		4	2000[e]	0.6[h]	0.5
29	612, 656	4.5	4	3100[f]	1.0[g]	0.8
	(0.553, 0.305)		6	1800[e]	0.5[i]	0.7

[a] Doping level 4%, at 10 V. [b] Weak electrofluorescence at ~440 nm from CBP was also observed. [c] At 10 V. [d] At 11 V. [e] At 12 V. [f] At 13 V. [g] At 20 mA cm^{-2}. [h] At 30 mA cm^{-2}. [i] At 50 mA cm^{-2}.

Electrophosphorescence: Application as OLED Emitters. Several platinum complexes were incorporated into multilayer OLEDs and yellow to red electroluminescence was generated. The devices in the present study were fabricated on indium-tin-oxide (ITO) glass using the vacuum deposition method. For comparison purposes, the multilayer device configuration reported by Thompson and Forrest was adopted.[10c] Generally, NPB (*N*,*N*′-di-1-naphthyl-*N*,*N*′-diphenyl-benzidine) and Alq_3 were used as the hole- and electron-transporting layers, respectively. BCP (2,9-dimethyl-4,7-diphenyl-1,10-phenanthroline, bathocuproine) was used to confine excitons within the luminescent zone, and magnesium silver alloy was used as the cathode. The Pt(II) σ-alkynyl materials were doped into the conductive host material CBP (4,4′-*N*,*N*′-dicarbazole-biphenyl) with mass ratios of 2 to 6%.

The performances of the OLEDs using Pt(II) σ-alkynyl complexes as electrophosphorescent materials are listed in Table 3 (see Figure 12 and Supporting Information for details of current density, voltage and luminance characteristics). Upon stimulation of positive bias voltage above ~4 V for devices with emitter ratios of 4 and 6%, intense orange to red emission

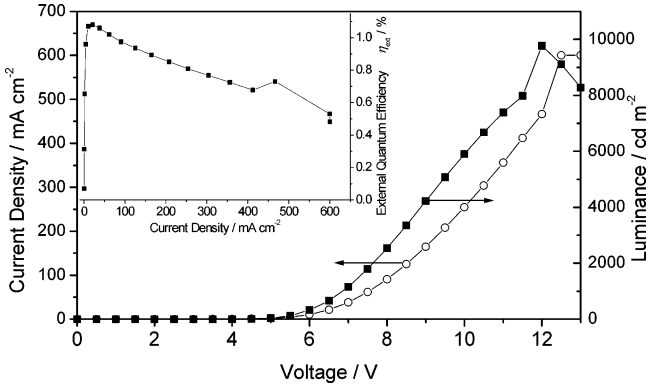

Figure 12. Current density, voltage and luminance characteristics (inset: external quantum efficiency vs current density) for OLED using **7** as emitter at 4% doping level.

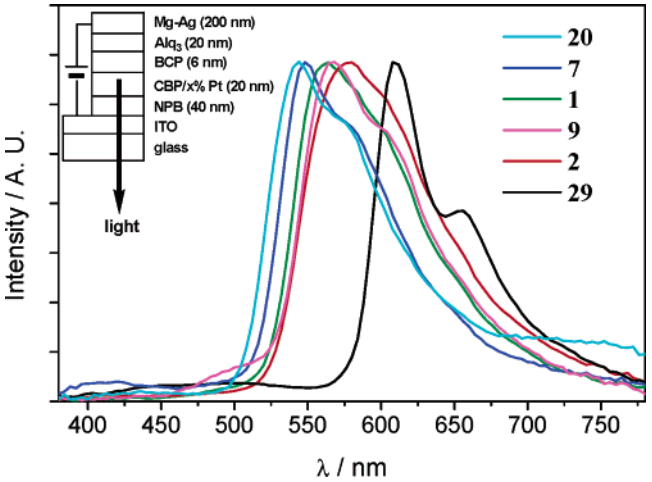

Figure 13. Normalized electroluminescence spectra for **1**, **2**, **7**, **9**, **20**, and **29** (4%) operated at 10 V.

is observed for **1**, **2**, **7**, **20**, **28**, and **29**, while blue emission from the host and hole-transporting layers is negligible. For **1**, **2**, **7**, **28**, and **29**, the emission maxima are independent of the doping level and applied voltage (for current density up to 600 mA cm^{-2}). As shown in Figure 13, the EL red-shifts in the order **7**, **1**, **2**, **9**, which is consistent with that observed for the photoluminescence (PL) in solution. For **1**, **2**, **7**, and **20**, the EL maximum is consistently blue-shifted by ca. 500 cm^{-1} from the PL values recorded in CH_2Cl_2 solution at 298 K. For **7** and **20**, both of which bear the pentafluorophenylacetylide ligand, doping levels of greater than 5% afford an additional broad emission at λ_{max} ca. 710 nm in the EL spectra. For **33**, both the blue emission of the host material CBP at λ_{max} ca. 440 nm and red emission with peak maxima at 620 and 670 nm were observed at 6% doping level.

The highest luminance (9800 cd m^{-2} at 12 V; λ_{max} 548 nm; CIE coordinates $x = 0.440$, $y = 0.506$) and EL efficiency [3.2 cd A^{-1} (η_{ext} 1.1%) at 20 mA cm^{-2}] are achieved by using emitter **7** at 4% doping level. The luminance of 7800 cd m^{-2} at 11 V and efficiency of 2.4 cd A^{-1} (η_{ext} 0.9%) at 30 mA cm^{-2} are obtained for an orange OLED (λ_{max} 564 nm; CIE coordinates $x = 0.480$, $y = 0.484$) using **1** at 4% doping level. At 2% ratio of **1**, improved luminance (9900 cd m^{-2} at 12 V) and efficiency [4.2 cd A^{-1} (η_{ext} 1.6%) at 30 mA cm^{-2}] are observed, but weak emission from CBP at λ_{max} ca. 440 nm is also detected. For the red OLED (λ_{max} 612 (max), 656 nm; CIE coordinates $x = 0.594$, $y = 0.341$), the maximum luminance of 3100 cd m^{-2} at 12 V and efficiency of 1.0 cd A^{-1} (η_{ext} 0.8%) at 30 mA cm^{-2} are observed using 4% of **29** in CBP. Generally, higher doping ratios led to lower efficiencies and inferior performance, apparently due to aggregate-induced quenching.

Discussion

General Remarks. The synthetic methodology to the tridentate cyclometalated Pt(II) σ-alkynyl complexes in the present study involves three steps. Hence, Kröhnke's method for oligopyridines,[22] Constable's cyclometalation process[24] and Sonogashira's metal-alkynyl formation reaction[1] have been adopted to prepare the cyclometalating ligand, its cyclometalated Pt(II) chloride derivative and the σ-alkynyl complexes, respectively. These procedures are generally efficient and tolerate a variety of substituents on the cyclometalating ligand, and such versatility facilitate the rational design and derivatization of this class of materials.

The structural determinations confirm the molecular structures of these complexes and in particular the presence of the Pt-alkynyl linkages. Intermolecular interactions in the crystal lattices of Pt(II) complexes are known to play a crucial role in their solid-state emission properties.[34] A variety of weak contacts, including $\pi-\pi$ stacking, Pt···Pt and C−H···F−C interactions, are revealed in the crystal structures of **1**, **2**, **7**, **8**, and **10**−**12**, and these may be invoked to rationalize the lower-energy solid-state emissions displayed by these complexes.

Consequence of the σ-Alkynyl Moiety: π-Conjugation with Pt(II). There are numerous reports on the phenomenon of π-conjugation in monomeric and oligomeric/polymeric trans-$Pt(C{\equiv}CR)_2$ moieties.[35] In the present work, we found that the acetylide ligand can affect the electronic structure of the complex, as reflected by both electrochemical and photophysical data. Complex **6** is an illustrative example, whereby the introduction of a nitro group at the 4-position of phenylacetylide leads to an increase in the $E^{1/2}$ value of the first reduction wave (by 0.2 V) that occurs primarily at the (C^N^N) ligand. If there is no communication between the arylacetylide and (C^N^N) groups, such an effect would be unlikely. We conceive that there is a degree of interaction between the π orbitals of the (C^N^N) and arylacetylide moieties via the Pt dπ orbitals, and hence the electron-withdrawing capability of the nitro group extends across the arylacetylide moiety and Pt(II) center and influences the redox nature of the (C^N^N) ligand. In the crystal structures, the small dihedral angles (5−7°) between the (C^N^N) and phenylacetylide planes in **2** and **7** suggest that favorable π-overlap can occur, while the larger dihedral angles for **1** (56°) and **8** (44°) still allow the possibility for partial π-overlap, although crystal packing effects cannot be disregarded.

There are apparently two transitions embedded in the allowed low-energy broad absorption band (in the 400−550 nm range)

(34) (a) Miskowski, V. M.; Houlding, V. H. *Inorg. Chem.* **1989**, *28*, 1529−1533. (b) Miskowski, V. M.; Houlding, V. H. *Inorg. Chem.* **1991**, *30*, 4446−4452. (c) Houlding, V. H.; Miskowski, V. M. *Coord. Chem. Rev.* **1991**, *111*, 145−152. (d) Miskowski, V. M.; Houlding, V. H.; Che, C. M.; Wang, Y. *Inorg. Chem.* **1993**, *32*, 2518−2524. (e) Bailey, J. A.; Hill, M. G.; Marsh, R. E.; Miskowski, V. M.; Schaefer, W. P.; Gray, H. B. *Inorg. Chem.* **1995**, *34*, 4591−4599.

(35) (a) Wilson, J. S.; Chawdhury, N.; Al-Mandhary, M. R. A.; Younus, M.; Khan, M. S.; Raithby, P. R.; Köhler, A.; Friend, R. H. *J. Am. Chem. Soc.* **2001**, *123*, 9412−9417 and references therein. (b) Liu, Y.; Jiang, S.; Glusac, K.; Powell, D. H.; Anderson, D. F.; Schanze, K. S. *J. Am. Chem. Soc.* **2002**, *124*, 12 412−12 413.

of these tridentate cyclometalated Pt(II) σ-alkynyl complexes, and one of these is likely to be the ^{1}MLCT (L = cyclometalating ligand) transition. The other transition apparently involves the σ-alkynyl group, since [(C^N^N)PtCl] and related derivatives without the acetylide auxiliary show only one transition in this spectral region with smaller extinction coefficients. Because the $^1\pi\pi^*$ transitions of arylacetylide metal complexes usually occur at significantly higher energies, the 'second' low-energy transition in these complexes is tentatively attributed to acetylide-to-(C^N^N) L′LCT or acetylide-to-platinum(II) LMCT transitions. We believe that the π-interaction across the Pt(II) center is crucial to the unusual physical and spectroscopic nature of these complexes.

Nature of Excited States and Substituent Effects. In our previous studies,[16] the emission of the [(C^N^N)PtCl] precursor and the cationic [(C^N^N)PtL]$^+$ (L = pyridine, phosphine or isocyanide) species are assigned to ^{3}MLCT (L = C^N^N) excited states and the broad low-energy absorption bands in the 380−420 nm range are attributed to ^{1}MLCT transitions. The introduction of an acetylide ligand into the [(C^N^N)Pt]$^+$ moiety makes such assignments more complicated, since arylacetylide and oligoynyl ligands also feature low-lying π and π^* orbitals that can participate in low-energy electronic transitions. The lowest-energy transitions of α-diimine platinum(II) bis(acetylide) complexes are typically ascribed to ^{3}MLCT [Pt(5d) → π^*(α-diimine)], but the involvement of ^{3}IL transitions for bis(4-nitrophenylacetylide) and bis(σ-phenylbutadiynyl) derivatives have also been proposed by Eisenberg[6b] and Che.[7] Recent studies on related luminescent terpyridine platinum(II)[36] and α-diimine rhenium(I)[37] complexes with extended σ-oligoynyl groups, plus theoretical calculations[38] on the α-diimine platinum(II) bis(acetylide) system, suggest that acetylide-to-diimine L′LCT transitions may contribute toward their emissive excited states. In the present work, we ascribe the lower-energy band in the absorption spectra to an allowed MLCT (L = diimine) transition. This assignment is consistent with the fact that the absorption band is red-shifted by electron-rich acetylide and electron-deficient (C^N^N) moieties and exhibits negative solvatochromism (i.e., transition energy increases with greater solvent polarity). Here, it is assumed that the energies of nonbonding and weakly π-bonding metal orbitals will increase with the donor strength of the arylacetylide ligands and that the ground state is more polar than the MLCT excited state. Accordingly, the emissions of **1**−**27** (see exceptions below) in fluid solution are assigned to ^{3}MLCT [Pt(5d) → π^*(cyclometalating ligand)] excited states in nature, in view of their solvent-sensitive emission energies and microsecond-regime lifetimes. It is noteworthy that, (1) the emission for [(C^N^N)PtC≡CC_6H_4-4-NO_2] (**6**) in alcoholic glass at 77 K (λ_{max} 537 nm; structured with vibronic progression of ∼1200 cm^{-1}) resembles the ^{3}IL(4-nitrophenylacetylide) emission of [(Cy_3P)AuC≡CC_6H_4-4-NO_2] in CH_2Cl_2 solution which appears at λ_{max} 524 nm;[39] and (2) the emission energy recorded in CH_2Cl_2 solution (λ_{max} 560 nm) for **6** is close to the reported ^{3}IL(4-nitrophenylacetylide) emission of [(4,4-^{t}Bu_2bpy)Pt(C≡CC_6H_4-4-NO_2)$_2$] at λ_{max} 570 nm. Therefore a triplet excited state composed of an admixture of ^{3}MLCT (L = C^N^N) and ^{3}IL-(4-nitrophenylacetylide) is assigned for **6**. Although complexes **6** and [(C^N^N)PtC≡CC_6F_5] (**7**) exhibit emissions at a similar energy (both at λ_{max} 560 nm) in CH_2Cl_2 at 298 K, the contribution from the ^{3}MLCT (L = C^N^N) excited state to the emission is expected to be greater for **7**, because the ^{3}IL-(C≡CC_6F_5) emission of [(Cy_3P)AuC≡CC_6F_5] occurs at λ_{max} ca. 485 nm in alcoholic glasses at 77 K, and this complex is nonemissive in fluid solution.[39]

The impact of the substituent at the 4-position of the (C^N^N) ligand upon the emission energy of the Pt(II) complexes has been evaluated. The emission is blue-shifted by electron-donating groups and red-shifted by electron-withdrawing moieties, and this is perfectly consistent with a MLCT (L = cyclometalating ligand) assignment for the excited state. Attachment of substituted phenyl groups at the 4-position (**14**−**18**) and functional groups on the cyclometalating phenyl moiety (**24**−**27**) does not dramatically alter the emission properties of these complexes. The minimal differences observed for the phenylacetylide derivatives **14**−**18** and **24**−**27** contrast directly with the remarkable substituent effects reported for the [Ir-(C^N)$_2$(acac)] system.[10d] The origins for these emissions are different; the photoluminescence of the former in fluid solution is derived from ^{3}MLCT excited states while that of the latter is predominantly ^{3}IL in nature.

A change in the emissive origin is apparent for lumophores supported by the heteroatom-containing (S^N^N) and (O^N^N) ligands. The fluid emissions [λ_{max} 616 and 644 nm in CH_2Cl_2 for the (S^N^N) (**28**−**30**) and (O^N^N) (**31**−**33**) series, respectively] occur at lower energies than their related (C^N^N) complexes. More importantly, the salient difference compared with the (C^N^N) series is that these emissions are *insensitive* to the substituent(s) on the arylacetylide ligand, although negative solvatochromic effects are detected (see Supporting Information for spectra of **28** and **33**). The excited states for these complexes are therefore tentatively assigned to ^{3}IL (L = S^N^N and O^N^N, respectively) charge-transfer transitions.

Narrow-Bandwidth Acetylenic $^3\pi\pi^*$ Emissions. Upon ascending the homologous series for [(C^N^N)Pt(C≡C)$_n$$SiMe_3$] ($n$ = 1−4, **10**−**13**), participation of the acetylide manifold in the electronic transitions is enhanced. Although the σ-donating abilities of the oligoynyl moieties in **10**−**13** are assumed to be comparable, the extension of the π-conjugation length may afford an energetically accessible acetylenic $^3\pi\pi^*$ state localized on the [−(C≡C)$_4$−] unit, the energy of which may be close to or even lower than that of the [Pt(C^N^N)] ^{3}MLCT state (typically ca. λ_{max} 560 nm). The intriguing vibronically structured narrow-width emission from **13** in fluid solution is similar to that of [(Cy_3P)Au(C≡C)$_4$Au(PCy_3)][31] in CH_2Cl_2 and identical to that of [(^{t}Bu_3tpy)Pt(C≡C)$_4$Pt(^{t}Bu_3tpy)](PF_6)$_2$ (^{t}Bu_3tpy = 4,4′,4″-tris-*tert*-butyl-2,2′:6′,2″-terpyridine) in CH_3CN, both in energy and vibronic progression, and this clearly indicates an acetylenic $^3\pi\pi^*$ excited state originating from the octatetraynyl ligand. Observation of localized acetylenic $^3\pi\pi^*$ emission from the −(C≡C)$_4$− moiety is feasible since it is lower in energy than the ^{3}MLCT state of the [Pt(C^N^N)] lumophore. The energy difference between these two triplet excited states is

(36) Yam, V. W. W.; Wong, K. M. C.; Zhu, N. *Angew. Chem., Int. Ed.* **2003**, *42*, 1400−1403.
(37) Yam, V. W. W.; Chong, S. H. F.; Ko, C. C.; Cheung, K. K. *Organometallics* **2000**, *19*, 5092−5097.
(38) (a) Klein, A.; van Slageren, J.; Záliš, S. *Inorg. Chem.* **2002**, *41*, 5216−5225. (b) van Slageren, J.; Klein, A.; Záliš, S. *Coord. Chem. Rev.* **2002**, *230*, 193−211. (c) Klein, A.; van Slageren, J.; Záliš, S. *Eur. J. Inorg. Chem.* **2003**, 1927−1938.
(39) See Supporting Information and: Lu, W.; Zhu, N.; Che, C. M. *J. Am. Chem. Soc.* **2003**, *125*, 16 081−16 088.

evidently small and hence three types of progressions (1360, 2150 and 2115 cm^{-1}) corresponding to the ground-state vibrations of the (C^N^N) and octatetraynyl ligands are detected in the emission spectrum of **13** in alcoholic glassy solution at 77 K (Figure 7). The observation of multiple and site-selective emissions signify that the octatetraynyl $^3\pi\pi^*$ and ^{3}MLCT (L = C^N^N) excited states may not be coupled in glassy solutions and their relative energies and decay pathways are presumably affected by the local micro-environment.

Interestingly, a red-shifted narrow-bandwidth emission is also observed for complex **21** in degassed fluid solutions, and this is attributed to a $^3\pi\pi^*$ excited state localized on the 1-ethynylpyrene ligand that is even lower in energy compared to the octatetraynyl unit. Nevertheless, as in the case of complex **13**, a small contribution from Pt(5d) $\rightarrow \pi^*$(alkynyl) excited-state cannot be excluded, in view of the red-shift from the gold-(I) congener [(Cy_3P)AuC≡Cpyrenyl-1] and the observed mild solvatochromism. Hence, the ligation of the octatetraynyl or 1-ethynylpyrene unit, both of which exhibit triplet $\pi \rightarrow \pi^*$-(alkynyl) excited states that are lower in energy compared to [(C^N^N)Pt] moieties, substantially changes the nature of the emissive excited state for the [(C^N^N)Pt(C≡C)$_n$R] lumophores.

MLCT Phosphors as OLED Emitters. If an emitter is intended for incorporation into a high-performance OLED where the thickness of each layer requires precise control to obtain charge balance, this material must tolerate the harsh conditions during vacuum-deposition processes. The tridentate cyclometalated Pt(II) complexes in the present study possess superior thermal stability when compared to bidentate aromatic α-diimine Pt(II) bis(arylacetylides) and other metal-alkynyl complexes that are also emissive but which easily decompose during vacuum deposition.[40] We suggest that π-conjugation of the tridentate aromatic ligand with the Pt-acetylide moiety may impart sublimability and additional stability to these neutral materials.

In devices with emitter ratios above 2% for **1**, **2**, **7**, **9**, **20**, **28**, and **29**, intense orange to red emission is observed while blue emission from the host and hole-transporting layers is negligible, implying efficient energy transfer from singlet to triplet excitons. However, for those devices with emitter ratio of 2% and for **33** as emitter at doping levels as high as 6%, both the blue EL of CBP at ca. 440 and orange-red EL are observed. This may be accredited to incomplete energy transfer from the CBP host to the triplet emitter. An additional broad EL band at λ_{max} 710 nm for devices with **7** and **20** as emitter at doping levels higher than 5% is tentatively ascribed to exciplex formation through C−H···F−C interactions between pentafluorophenylacetylide moieties and the host CBP molecules.

The color of the ^{3}MLCT (L = C^N^N) emission for the [(C^N^N)PtC≡CR] series can be tuned from green to orange-red by chemical modification of both the tridentate cyclometalating and arylacetylide ligands, while the ^{3}IL (L = S^N^N and O^N^N) emissions occur in the red region. The emission tunability, microsecond-scale lifetime plus their superior thermal stability renders this class of lumophores suitable as electrophosphorescent dopants in OLED applications. The resultant electroluminescent spectra resemble their photoluminescent counterparts recorded in solution. For devices employing (C^N^N)-based emitters, blue-shifted EL energies (by ca. 500 cm^{-1}) were observed, while the EL energies for (S^N^N)-based emitters are virtually identical (a slight blue shift of less than 100 cm^{-1}) to the PL values recorded in solution. It is well-known that ^{3}MLCT excited states are environment-sensitive and exhibit hypsochromism in a rigid matrix.[41] If we regard the emitting layer of an electroluminescent device as a rigid matrix of dispersed phosphorescent dopant molecules, the blue shift of the EL energy relative to the PL is not surprising.

Summary and Prospects

Our results demonstrate that the present class of tridentate cyclometalated Pt(II) σ-alkynyl complexes exhibit highly emissive excited states that can be ^{3}MLCT, $^3\pi\pi^*$(alkynyl) and/or ^{3}IL(cyclometalating ligand) in nature, and the relative energies of the Pt d-orbitals and the π and π^* orbitals of the cyclometalating and σ-alkynyl ligands ultimately govern their emissive characteristics. It is noteworthy that the σ-alkynyl component in our complexes can act as photophysically 'active' ligands and constitute an integral part of the electronic structure through Pt−(alkynyl) π-conjugation, so that another approach to fine-tune the emissive properties of metal-based phosphorescent emitters becomes available. Significantly, low-energy narrow-bandwidth emissions from acetylenic $^3\pi\pi^*$ excited states localized on the −(C≡C)$_4$− and 1-ethynylpyrene auxiliaries are observed in fluid solutions.

The tridentate cyclometalated Pt(II) σ-alkynyl complexes are promising light-emitting materials, especially as phosphorescent dopants for OLED applications, due to their intense, readily adjustable triplet emissions under ambient conditions and their thermal stability. For the ^{3}MLCT emitters of the series, the EL is slightly blue-shifted from the PL recorded in fluid solution, and this should be taken into account when designing colors for a multicolor OLED display. Because EL energies can be fine-tuned through chemical modification of both the tridentate cyclometalating and σ-alkynyl auxiliaries, it may be feasible to develop high-efficiency and -brightness multicolor OLEDs based on these organometallic emitters. A high-throughput combinatorial approach[42] is anticipated to be a more efficient method to achieve high-performance emitters based on the chemistry and photo- and electroluminescence reported here. Indeed, there remains significant scope for optimization of device fabrication and OLED performance.

Experimental Section

General Procedures and Materials. All starting materials were purchased from commercial sources and used as received unless stated otherwise. The solvents used for synthesis were of analytical grade. The compounds 4-nitrophenylacetylene,[43] pentafluorophenylacetylene,[44] Ph(C≡C)$_2$H,[45] $Me_3Si(C{\equiv}C)_2H$,[46] $Me_3Si(C{\equiv}C)_nSiMe_3$ (n = 3,[25] 4[26]), 1-ethynylpyrene[47] and [(C^N^N)PtCl] (HC^N^N = 6-phenyl-2,2′-bipyridine)[24] and [(S^N^N)PtCl] (HS^N^N = 6-(2-thienyl)-2,2′-bipyridine)[24] were prepared following literature methods. The compound

(40) Ma, Y. G.; Chan, W. H.; Zhou, X. M.; Che, C. M. *New J. Chem.* **1999**, 263−265.

(41) (a) Wrighton, M.; Morse, D. L. *J. Am. Chem. Soc.* **1974**, *96*, 998−1003. (b) Lees, A. J. *Comment. Inorg. Chem.* **1995**, *17*, 319−346.
(42) Lavastre, O.; Illitchev, I.; Jegou, G.; Dixneuf, P. H. *J. Am. Chem. Soc.* **2002**, *124*, 5278−5279.
(43) Takahashi, S.; Kuroyama, Y.; Sonogashira, K.; Hagihara, N. *Synthesis* **1980**, 627−630.
(44) Zhang, Y. D.; Wen, J. X. *Synthesis* **1990**, 727−728.
(45) Kende, A. S.; Smith, C. A. *J. Org. Chem.* **1988**, *53*, 2655−2657.
(46) Bartik, B.; Dembinski, R.; Bartik, T.; Arif, A. M.; Gladysz, J. A. *New J. Chem.* **1997**, *21*, 739−750.
(47) Inouye, M.; Hyodo, Y.; Nakazumi, H. *J. Org. Chem.* **1999**, *64*, 2704−2710.

1-(2-furyl)-3-dimethylaminopropan-1-one hydrochloride was obtained by refluxing a mixture of 2-acetylfuran, $Me_2NH{\cdot}HCl$ and paraformaldehyde in ethanol. ^1H and ^{13}C NMR spectra were recorded on a Bruker Avance 400 or 300 DRX FT-NMR spectrometer (referenced to residual solvent) at 298 K. ^{19}F NMR spectra were recorded on a Bruker Avance 400 (trifluoroacetic acid reference) at 298 K. Mass spectra (FAB) were obtained on a Finnigan MAT 95 mass spectrometer. Elemental analyses were performed by Beijing Institute of Chemistry, Chinese Academy of Sciences. X-ray crystallographic data were collected on a MAR diffractometer with a 300 mm image plate detector using monochromatized Mo Kα radiation ($\lambda = 0.710\ 71$ Å). Details of solvent treatment for photophysical studies and cyclic voltammetric studies have been described earlier.[7]

UV−vis spectra were recorded on a Perkin-Elmer Lambda 19 UV−vis spectrophotometer. Solution samples for emission measurements were degassed by at least four freeze−pump−thaw cycles. Emission spectra were obtained on a SPEX Fluorolog-2 Model F111 fluorescence spectrophotometer. Emission lifetime measurements were performed with a Quanta Ray DCR-3 pulsed Nd:YAG laser system (pulse output 355 nm, 8 ns). Luminescent quantum yields were referenced to $[Ru(bpy)_3](ClO_4)_2$ in acetonitrile ($\phi = 0.062$) and extrapolated to infinite dilution (estimated error ± 15%). Self-quenching studies were performed by luminescence lifetime measurements over a range of complex concentrations (5×10^{-6} to 5×10^{-4} M) and fitted by a modified Stern−Volmer expression (eq 1)[48]

$$\tau_0/\tau_{obs} = 1 + k_q\tau_0[Pt] \quad (1)$$

where k_q is the self-quenching rate constant, [Pt] is the concentration of Pt complex, and τ_0 and τ_{obs} are the lifetime of the lumophore in infinite dilution and known concentration, respectively. The radiative and nonradiative rate constants were calculated using eq 2 and 3, respectively

$$k_r = \phi_0{\tau_0}^{-1} \quad (2)$$

$$k_{nr} = k_r({\phi_0}^{-1} - 1) \quad (3)$$

where k_r and k_{nr} are the radiative and nonradiative rate constant, respectively, ϕ_0 and τ_0 are the luminescence quantum yield and lifetime of the lumophore in infinite dilution, respectively. Transient absorption spectra were performed with the mentioned Nd:YAG laser system with pulse-width of 8 ns. 355 nm output (third harmonic) was used. The monitoring light was from a 300 W continuous wave tungsten−halogen or xenon lamp oriented orthogonally to the direction of the laser pulse. Transient species was monitored by the monochromatic light from tungsten or xenon lamp. The transient absorption signals at individual wavelengths were fed to the Tektronix 2430 or TDS 350 oscilloscope. The entire optical difference spectrum was generated point to point by monitoring at each wavelength.

OLED Fabrication and Characterization. Devices were fabricated with the following configuration: glass/indium tin oxide (ITO: 30 Ω/square)/NPB (400 Å)/CBP doped with tridentate cyclometalated Pt(II) σ-alkynyl complex (60 Å)/Alq_3 (200 Å)/Mg:Ag (2000 Å). The ITO glass substrate was cleaned with detergent and deionized water and dried in an oven for 2 h. It was then treated with UV-ozone for 25 min before loading into a deposition chamber. The organic films of NPB, CBP:Pt complex, BCP and Alq_3 were sequentially deposited onto the ITO substrate at a pressure of around 1.0×10^{-5} mbar. The pressure during deposition of the Pt(II) complex was maintained below 9.0×10^{-6} mbar to minimize decomposition. The current-voltage-luminance characteristics and EL spectra were recorded with a computer-controlled DC power supply and a Spectrascan PR650 photometer at room temperature. The emission area of the devices is 0.1 cm^2, as defined by the overlapping area of the anode and cathode. The external quantum efficiencies η_{ext} were calculated based on the method described by Okamoto et al.[49] using luminance, EL spectrum and current density.

Acknowledgment. We are grateful for financial support from The University of Hong Kong, the Research Grants Council of Hong Kong SAR, China [HKU 7039/03P and CityU 8730009], the Croucher Foundation (Hong Kong), and the Innovation and Technology Commission of the Hong Kong SAR Government (ITS/053/01). W.L. acknowledges the receipt of his studentship from The University of Hong Kong. We thank Mr. Wai-Lim Chan for assistance in device fabrication and Dr. Kung-Kai Cheung for solving the crystal structure of complex **10**.

Supporting Information Available: Synthesis and characterization data; TGA curves for **1** and **28**; additional crystallographic plots and CIFs; supplementary absorption and emission spectra; cyclic voltammograms; configuration, current density, voltage and luminance characteristics of selected OLEDs. This material is available free of charge via the Internet at http://pubs.acs.org.

JA0317776

(48) Vincze, L.; Sandor, F.; Pem, J.; Bosnyak, G. *J. Photochem. Photobiol. A* **1999**, *120*, 11−14.
(49) Okamoto, S.; Tanaka, K.; Izumi, Y.; Adachi, H.; Yamaji, T.; Suzuki, T. *Jpn. J. Appl. Phys.* **2001**, *40*, L783−L784.